

Effect of Ozone on CO₂ Assimilation and PSII Function in Plants with Contrasting Pollutant Sensitivities

Myoung Hui Yun

Dissertation Submitted to the Faculty of the Virginia Polytechnic Institute and State
University in partial fulfillment of the requirements for the degree of

DOCTOR OF PHILOSOPHY

in

Plant Physiology and Weed Science

APPROVED:

Dr. Boris I. Chevone, Chairperson

Dr. Anton Baudoin

Dr. John Hess

Dr. David Orcutt

NOT APPROVED:

Dr. John Seiler

March 12, 2007

Blacksburg, Virginia

Key Words: Black cherry, Tobacco, Ozone, Foliar Visible Injury, Gas Exchange,
Photosynthetic Activity, Chlorophyll Fluorescence

Effect of Ozone on CO₂ Assimilation and PSII Function in Plants with Contrasting Pollutant Sensitivities

Myoung Hui Yun

(Abstract)

Ozone is known to be the most widespread phytotoxic air pollutant. Ozone causes visible injury, reductions in photosynthesis, growth, and yield. Plant response to ozone may vary with species, varieties, and physiological age. Comparison between sensitive and tolerant cultivars has a key role in assessing ozone damage, investigating the sites of cellular injury, and identifying ozone tolerance mechanism. The objectives of this study were to investigate the effects of high ozone concentration (200 ppb) as well as ambient ozone concentrations (under field conditions) on net CO₂ assimilation and PSII function in plants with different sensitivities to ozone. Two species of plants, tobacco (*Nicotiana tabacum* L.) and black cherry (*Prunus serotina*) were studied. Gas exchange analysis and chlorophyll fluorometry were utilized to characterize physiological function.

Two tobacco cultivars, Bel-B and Bel-W3, tolerant and sensitive to ozone, respectively, were grown in a greenhouse supplied with charcoal filtered air and then exposed to 200 ppb ozone for 4hr. Effects on chlorophyll fluorescence, net photosynthesis, and stomatal conductance are described. Quantum yield was calculated from chlorophyll fluorescence and the initial slope of the assimilation-light curve measured by the gas exchange method. Only the sensitive cultivar, Bel-W3, developed visible injury symptoms involving up to 50% of the 5th leaf. The maximum net photosynthetic rate of ozone-treated plants of the tolerant cultivar was reduced 40% compared to control plants immediately after ozone fumigation; however, photosynthesis recovered by 24 hr post fumigation and remained at the same level as control plants. In the sensitive cultivar, on the other hand, ozone exposure reduced maximum net photosynthesis up to 50%, with no recovery, apparently causing permanent damage to the photosystem. Reductions in apparent quantum efficiency, calculated from the assimilation-light curve, differed between cultivars. Bel-B showed an immediate depression of 14% compared to controls, whereas Bel-W3 showed a 27% decline. Electron transport rate (ETR), at

saturating light intensity, decreased 58% and 80% immediately after ozone treatment in Bel-B and Bel-W3, respectively. Quantum yield decreased 28% and 36% in Bel-B and Bel-W3, respectively. It can be concluded that ozone caused a greater relative decrease in linear electron transport than maximum net photosynthesis, suggesting greater damage to PSII than the carbon reduction cycle.

Two different sensitivity classes of black cherry, tolerant and sensitive, growing under natural environmental conditions in Giles County, VA were assessed for physiological responses to ambient ozone concentrations. Additional measurements were made at two other sites near Blacksburg. Leaf gas exchange rates and visible foliar injury were determined monthly during the growing seasons of 2000, 2001, and 2002 to characterize the relationship of injury to altered photosynthetic function. Ambient ozone levels were sufficient to induce visible symptoms which were highly correlated with a reduction in Pn_{MAX} (maximum net photosynthetic rate under saturating light conditions) and ΦCO_2 (quantum yield for carbon reduction) only in sensitive black cherry. Electron transport rate (ETR) and quantum yield of PSII ($\Phi PSII$) were also reduced in sensitive black cherry. Maximum photochemical efficiency (Fv/Fm) in sensitive trees was severely damaged by ambient ozone. There were positive correlations between increasing cumulative ozone concentration and substantial reductions in Pn_{MAX} and in ΦCO_2 of sensitive trees compared to tolerant trees. There was a negative correlation between chlorophyll content and percent leaf injury in sensitive black cherry.

DEDICATION

To my husband and daughter

To my parents

Acknowledgement

First of all, my utmost thanks go to God for providing and leading my life and giving me strength and opportunity to accomplish this dissertation.

I would like to express my sincere gratitude to my advisor, Dr. Chevone, for his continuous guidance, inspiration, encouragement, invaluable help and patience. I would also like to express sincere thanks to Drs Anton Baudoin, John Hess, David Orcutt, and John Seiler for serving on my committee and providing valuable guidance and encouragement. They sacrificed their time to make this dissertation more readable and my arguments intelligible. I'm also grateful to Dr. Cindy Denbow for her generous support in my difficult time.

I would like to thank Moonsun Jeong, Yeasun Chung, SoYeon Park and many other great people I met at Virginia Tech for their help and friendship.

Last but not least, I would like to express special thanks to my parents, Ki-soon Yun and Chanuk Lee, my loving husband, Kanguk, and my dearest daughter, Yoonha, for their profound love, understanding, sacrifices, and tremendous support which made my education and scientific endeavor possible.

Table of Contents

Chapter 1	1
Introduction	1
Chapter 2	8
Ozone Alters CO₂ Exchange rates and Chlorophyll Fluorescence in Two Tobacco cultivars (<i>Nicotiana tabacum</i>) with different sensitivities	8
2.1 Introduction	8
2.2 Materials and Methods	10
2.2.1 Plant material and growth conditions	10
2.2.2 Ozone exposure	10
2.2.3 Visible injury	10
2.2.4 Net photosynthesis	10
2.2.5 Chlorophyll fluorescence	11
2.2.6 Experimental design and statistical analysis	12
2.3 Results	12
2.3.1 Photosynthetic function in control plants	12
2.3.2 Visible foliar symptoms	13
2.3.3 Photosynthetic function in ozone-treated plants	14
2.3.4 Chlorophyll fluorescence in control and ozone-treated plants	22
2.4 Discussion	22
2.4.1 Effects of high concentration of ozone on tobacco	22
Chapter 3	30
Photosynthetic response of tolerant and sensitive black cherry (<i>Prunus serotina</i>) to ambient ozone concentrations under natural conditions	30
3.1 Introduction	30
3.2 Materials and Methods	32
3.2.1 Experimental site and design	32
3.2.2 Foliar visible injury and chlorophyll content	33
3.2.3 Net photosynthesis	34
3.2.4. Chlorophyll fluorescence analysis	36
3.2.5 Statistical analysis	36
3.3 Results	37
3.3.1 Ozone exposure	37
3.3.2. Correlations between cumulative ozone and photosynthetic activities	41

3.3.3. Physiological gas exchange	41
3.3.4. Visible foliar injury.....	48
3.3.5 Chlorophyll fluorescence	48
3.4 Discussion	58
Chapter 4	71
4.1 Conclusion	71
References	74
Appendix - I. Tables	86
Appendix – II. Symbols and units	90
Vita	91

List of Tables

Table 2.1 Maximum net photosynthetic rates (Pn_{MAX} , $\mu\text{mol CO}_2 \text{ m}^{-2} \text{ s}^{-1}$ at $900 \mu\text{mol m}^{-2} \text{ s}^{-1}$) in Bel-B (tolerant) and Bel-W3 (sensitive) tobacco cultivars after exposure to 200 ppb ozone for 4 hr. Single asterisk indicates significant differences from control plants at $P<0.05$. Values are means \pm s.d.	17
Table 2.2 Quantum yield for CO_2 assimilation ($\mu\text{mol CO}_2 \mu\text{mol photons}^{-1}$) in Bel-B and Bel-W3 tobacco cultivars after exposure to 200 ppb ozone for 4 hr. Single asterisk indicates significant differences from control plants at $P<0.05$, two asterisks indicate significant differences at $P<0.01$. Values are means \pm s.d.	18
Table 2.3 Stomatal conductance (g_s , $\text{mmol H}_2\text{O m}^{-2} \text{ s}^{-1}$) in Bel-B and Bel-W3 tobacco cultivars after exposure to 200 ppb ozone for 4 hr. Single asterisk indicates significant differences from control plants at $P<0.05$. Values are means \pm s.d.	19
Table 2.4 Fluorescence characteristics and the apparent electron transport rate (ETR) in leaves of Bel-B and Bel-W3 immediately after ozone fumigation at 200 ppb for 4 hr. Asterisks indicate significant differences from control plants at $P<0.05$. Values are mean \pm s.d.	25
Table 2.5. Summary of photosynthetic activities, gas exchange and chlorophyll fluorescence, before and after ozone fumigation in tobacco cultivars. Prior to ozone fumigation percentage reduction calculated as $(T-S)/T \times 100$ (T, tolerant; S, sensitive). With ozone fumigation, percentage reduction calculated as $(C-O)/C \times 100$ (C, control plants; O, ozone treated plants)	26
Table 3.1 Seasonal means of atmospheric ambient ozone concentrations (ppb) and seasonal cumulative ozone concentrations (ppm h) at HRC for three consecutive years, 2000 to 2002. Values are means \pm s.d.	38
Table 3.2 Maximum net photosynthetic rate (Pn_{MAX} , $\mu\text{mol CO}_2 \text{ m}^{-2} \text{ s}^{-1}$ at $900 \mu\text{mol m}^{-2} \text{ s}^{-1}$), stomatal conductance (g_s , $\text{mol H}_2\text{O m}^{-2} \text{ s}^{-1}$), internal CO_2 concentration (C_i , ppm) and apparent quantum yield for CO_2 assimilation (ΦCO_2 , $\mu\text{mol CO}_2 \mu\text{mol quanta}^{-1}$) on the 3 rd leaf of black cherry during the growing season of 2000, at HRC. Values are means \pm s.d. Asterisks indicate significant differences between phenotypes. * at $P<0.05$ and ** at $P<0.01$	45
Table 3.3 Maximum net photosynthetic rate (Pn_{MAX} , $\mu\text{mol CO}_2 \text{ m}^{-2} \text{ s}^{-1}$ at $900 \mu\text{mol m}^{-2} \text{ s}^{-1}$), stomatal conductance (g_s , $\text{mol H}_2\text{O m}^{-2} \text{ s}^{-1}$), internal CO_2 concentration (C_i , ppm) and apparent quantum yield for CO_2 assimilation (ΦCO_2 , $\mu\text{mol CO}_2 \mu\text{mol quanta}^{-1}$) on the 3 rd leaf of black cherry in June and September, 2001, at HRC. Values are mean \pm s.d. Asterisks indicate significant differences between phenotypes. ** at $P<0.01$	46

List of Tables

Table 3.4 Maximum net photosynthetic rate (Pn_{MAX} , $\mu\text{mol CO}_2 \text{ m}^{-2} \text{ s}^{-1}$ at $900 \mu\text{mol m}^{-2} \text{ s}^{-1}$), stomatal conductance (g_s , $\text{mol H}_2\text{O m}^{-2} \text{ s}^{-1}$), apparent quantum yield for CO_2 assimilation (ΦCO_2 , $\mu\text{mol CO}_2 \mu\text{mol quanta}^{-1}$), and carboxylation efficiency (ΦCE , $\mu\text{mol CO}_2 \text{ ppm CO}_2^{-1}$) on the 3 rd leaf of black cherry during growing season of 2002, at HRC. Values are means \pm s.d. Asterisks indicate significant differences between phenotypes. * at $P < 0.05$ and ** at $P < 0.01$.	47
Table 3.5 Percentage differences of photosynthetic activities (Pn_{MAX} , g_s , C_i , ΦCO_2 , and ΦCE) in sensitive black cherry compared to tolerant black cherry. Percentage differences were calculated as $(T-S)/T \times 100$ at three different sites MTR, APL, and HRC, 2000 to 2002.	49
Table 3.6 Parameters from the assimilation-irradiance (A-I) response curves of tolerant (T) and sensitive (S) black cherry during June to September for three years at HRC. A_{SAT} , assimilation at light saturation ($\mu\text{mol CO}_2 \text{ m}^{-2} \text{ s}^{-1}$ at $1800 \mu\text{mol photon m}^{-2} \text{ s}^{-1}$); LCP, light compensation point ($\mu\text{mol m}^{-2} \text{ s}^{-1}$); R_D , respiration during the day ($\mu\text{mol CO}_2 \text{ m}^{-2} \text{ s}^{-1}$). Values are means \pm s.d.	50
Table 4.1 Comparison of response of tobacco to acute ozone exposure with that of black cherry to chronic ozone exposure.	73
Table A.1 Gas exchange analysis was conducted during the growing seasons of 2000 to 2002 at three different sites MTR, APL, and HRC. Various photosynthetic activities (Pn_{MAX} , $\mu\text{mol CO}_2 \text{ m}^{-2} \text{ s}^{-1}$ at $900 \mu\text{mol m}^{-2} \text{ s}^{-1}$; g_s , $\text{mol H}_2\text{O m}^{-2} \text{ s}^{-1}$; C_i , ppm; ΦCO_2 , $\mu\text{mol quanta}^{-1}$; and ΦCE) on the 3 rd basal leaf were compared between tolerant (T) and sensitive (S) black cherry. Values are mean \pm s.d.	86
Table A.2 Chlorophyll fluorescence in the dark-adapted state (F_m , maximum fluorescence; F_o , initial fluorescence; and F_v/F_m , maximum photochemical efficiency), quantum yield for PSII (ΦPSII), maximum electron transport rate (ETR, $\mu\text{mol electron m}^{-2} \text{ s}^{-1}$ at $950 \mu\text{mol m}^{-2} \text{ s}^{-1}$), and quenching coefficients (q_P , photochemical quenching; q_N , non-photochemical quenching) on the 3 rd leaf of black cherry during growing season of 2000 at HRC. Values are means \pm s.d. Asterisks indicate significant differences between cultivars * at $P < 0.05$ and ** at $P < 0.01$.	87

List of Tables

Table A.3 Chlorophyll fluorescence in the dark-adapted state (F_m , maximum fluorescence; F_o , initial fluorescence; and F_v/F_m , maximum photochemical efficiency), quantum yield for PSII (Φ_{PSII}), maximum electron transport rate (ETR, $\mu\text{mol electron m}^{-2} \text{s}^{-1}$ at $950 \mu\text{mol m}^{-2} \text{s}^{-1}$), and quenching coefficients (qP, photochemical quenching; qN, non-photochemical quenching) on the 3 rd leaf of black cherry during the growing season of 2001 at HRC. Values are means \pm s.d. Asterisks indicate significant differences between cultivars * at $P < 0.05$ and ** at $P < 0.01$	88
Table A.4 Chlorophyll fluorescence in the dark-adapted state (F_m , maximum fluorescence; F_o , initial fluorescence; and $F_v \pm /F_m$, maximum photochemical efficiency), quantum yield for PSII (Φ_{PSII}), maximum electron transport rate (ETR, $\mu\text{mol electron m}^{-2} \text{s}^{-1}$ at $950 \mu\text{mol m}^{-2} \text{s}^{-1}$), quenching coefficients (qP, photochemical quenching; qN, non-photochemical quenching), and chlorophyll concentrations on the 3 rd leaf of black cherry during the growing season of 2002 at HRC. Values are means \pm s.d.....	89

List of Figures

- Figure 2.1** Net assimilation ($\mu\text{mol CO}_2 \text{ m}^{-2}\text{s}^{-1}$) - irradiance (PAR; $\mu\text{mol m}^{-2}\text{s}^{-1}$) on the 4th leaf position of control tobacco plants, Bel-B (BBC; open circles) and Bel-W3 (BWC; closed squares). Insert shows the initial slopes of the A-I response curves. Bars represent \pm one standard deviation and, where not apparent, are contained within the symbols. 15
- Figure 2.2** (A) Maximum net photosynthetic rate (Pn_{MAX} , $\mu\text{mol CO}_2 \text{ m}^{-2}\text{s}^{-1}$) (B) stomatal conductance (g_s , $\text{mmol H}_2\text{O m}^{-2}\text{s}^{-1}$), and (C) internal CO_2 concentration (C_i , ppm) in relation to leaf age in Bel-B (closed circles) and Bel-W3 (closed squares) (leaf 8 cm long at day 1) in nonfumigated plants. Arrow indicates the ozone fumigation and block indicates duration of experimental period. Bars represent \pm one standard deviation and, where not apparent, are contained within the symbols. Lines were fitted by polynomial (A) and linear (B) and (C) regression. 16
- Figure 2.3** Visible symptoms on the foliage 48 hr post-ozone-fumigation (200 ppb for 4 hr) in tobacco cultivars Bel-B (black bars) and Bel-W3 (white bars), (A) percentage of visible injury and (B) appearance of foliar injury on the 4th leaf position. 20
- Figure 2.4** (A) Percentage reduction of maximum net photosynthetic rates and (B) percentage reduction of quantum yield for CO_2 assimilation in Bel-B (black bars) and Bel-W3 (white bars) tobacco cultivars exposed to 200 ppb of ozone for 4 hr. Initial rates are taken from control plants at 0 hr post-ozone-fumigation. Bars represent one standard deviation. 21
- Figure 2.5** Percentage difference in dark adapted state chlorophyll fluorescence parameters F_o minimum chlorophyll fluorescence (black bars) F_m maximum chlorophyll fluorescence (grey bars) and $F_v[F_m-F_o]/F_m$ maximum photochemical efficiency of PSII (white bars) in Bel-B and Bel-W3 tobacco cultivars immediately after ozone fumigation of 200 ppb ozone for 4 hr. Bars represent one standard deviation. 23
- Figure 2.6** (A) electron transport rates of PSII (ETR, $\mu\text{mol electron m}^{-2}\text{s}^{-1}$) and (B) quantum efficiency for PSII (Φ_{PSII}) – Irradiance (PAR $\mu\text{mol m}^{-2}\text{s}^{-1}$) response curves on the 4th leaf in Bel-B (BBC, control plants and BBO, ozone treated plants) and Bel-W3 (BWC, control plants and BWO, ozone treated plants) tobacco cultivars immediately after ozone fumigation with 200 ppb of ozone for 4hr. Bars represent \pm one standard deviation. 24

List of Figures

Figure 3.1. Daily peaks of atmospheric ambient ozone concentration (ppb) at Horton Research Center (HRC), during the growing season of three consecutive years 2000 through 2002 39	39
Figure 3.2. Seasonal cumulative ozone concentrations (SUM00, ppm h) for three years 2000 to 2002 at HRC.	40
Figure 3.3 Percent difference $[100 \times (T-S)/T]$ (A) in Pn_{MAX} (maximum net photosynthetic rate, $\mu\text{mol CO}_2 \text{ m}^{-2} \text{ s}^{-1}$ at $900 \mu\text{mol CO}_2 \text{ m}^{-2} \text{ s}^{-1}$) and (B) in apparent quantum yield for carbon reduction (ΦCO_2 , $\mu\text{mol CO}_2 \mu\text{mol quanta}^{-1}$) in sensitive black cherry compared to tolerant black cherry, as related to cumulative ozone concentration (ppm h). Data collected during the 2000 through 2002 growing seasons at HRC. $n=14$ for ΦCO_2 based on monthly measurements of light response curves. $n=31$ for Pn_{MAX} which includes a second Pn_{MAX} measurement every month.	42
Figure 3.4 Examples of net assimilation (Pn , $\mu\text{mol CO}_2 \text{ m}^{-2} \text{ s}^{-1}$) - C_i response curves (at $2000 \mu\text{mol m}^{-2} \text{ s}^{-1}$ PAR) on the 3rd leaf of sensitive (closed circles) and tolerant (open circles) black cherry during the growing season of 2002, at HRC. Bars represent \pm one standard deviation and, where not apparent, are contained within symbols.	51
Figure 3.5 Apparent leaf injury developed in sensitive trees in September, 2000 at MTB.	52
Figure 3.6 Percent visible foliar injury of total leaf area estimated on the different leaf positions of sensitive black cherry in September, 2001, at HRC. Leaf position 10 (L10) is the youngest leaf estimated. Bars represent one standard deviation.	53
Figure 3.7 Maximum net photosynthetic rate (Pn_{MAX} ; $\mu\text{mol CO}_2 \text{ m}^{-2} \text{ s}^{-1}$ at $900 \mu\text{mol m}^{-2} \text{ s}^{-1}$) on the different leaf positions of sensitive (closed circles) and tolerant (open circles) black cherry in September, (A) 2000 at APL and (B) 2001 at HRC. Leaf position 8 is the youngest leaf measured. Bars represent \pm one standard deviation and, where not apparent, are contained within symbols.	54
Figure 3.8 Pn_{MAX} (Maximum net photosynthetic rates, $\mu\text{mol CO}_2 \text{ m}^{-2} \text{ s}^{-1}$ at $900 \mu\text{mol m}^{-2} \text{ s}^{-1}$) in relation to percent visible foliar injury of sensitive black cherry in two consecutive years, 2000 (solid line and closed circles) and 2001 (dotted line and open circles), at HRC.	55
Figure 3.9 (A) Chlorophyll contents on the 3 rd leaf of sensitive (black bars) and tolerant (white bars) black cherry during the growing season of 2002, at HRC. (B) Chlorophyll content (mg/m^2), in relation to percent visible foliar injury in sensitive black cherry in September, 2002, at HRC. Percent visible injury estimated to the nearest 5%. Each point represents three samples. Bars represent one standard deviation. Asterisks indicate significant differences between phenotypes. * at $P < 0.05$ and ** at $P < 0.01$	56

List of Figures

- Figure 3.10.**(A) Maximum photochemical efficiency of PSII ($F_v [F_m - F_o]/F_m$; F_m , maximum fluorescence; F_o , minimum fluorescence) and (B) quantum efficiency for PSII (Φ_{PSII}) on the 3rd leaf of sensitive (closed circles) and tolerant (open circles) black cherry during the growing season, 2000, at HRC. Bars represent \pm one standard deviation. Asterisks indicate significant differences between phenotypes. * at $P < 0.05$ and ** at $P < 0.01$ 59
- Figure 3.11** (A) Maximum photochemical efficiency of PSII ($F_v[F_m - F_o]/F_m$; F_m , maximum fluorescence; F_o , minimum fluorescence), (B) electron transport rates of PSII (ETR, $\mu\text{mol electrons m}^{-2}\text{s}^{-1}$), and (C) non-photochemical quenching (qN) on the 3rd leaves of sensitive (closed circles and black bars) and tolerant (open circles and white bars) black cherry during the summer of 2001 at HRC. Bars represent \pm one standard deviation. Asterisks indicate significant differences between phenotypes. * at $P < 0.05$ and ** at $P < 0.01$ 60
- Figure 3.12** (A) Maximum photochemical efficiency of PSII ($F_v [F_m - F_o]/F_m$; F_m , maximum fluorescence; F_o , minimum fluorescence), (B) percentage changes in maximum photochemical efficiency ($F_v [F_m - F_o]/F_m$, white bars) and its components, maximum chlorophyll fluorescence (F_m , grey bars) and minimum chlorophyll fluorescence (F_o , black bars), and (C) quantum efficiency for PSII (Φ_{PSII}) on the 3rd leaf of sensitive (closed circles) and tolerant (open circles) black cherry during the growing season of 2002, at HRC. Bars represent \pm one standard deviation and, where not apparent, are contained within symbols. Asterisks indicate significant differences between phenotypes. * at $P < 0.05$ and ** at $P < 0.01$ 61

Chapter I

Introduction

Ozone (O₃) is considered to be the most phytotoxic among common air pollutants (Saitanis and Karandinos, 2002). As a secondary pollutant, ozone is formed by photolysis of nitrogen dioxide (NO₂) via a series of complex photochemical reactions (Schraudner *et al.*, 1997). Plant damage from ozone is most severe during the summer when maximum solar radiation occurs and plant growth is rapid. Adverse effects of ozone on plants include foliar symptoms such as, bronzing, chlorosis, bifacial necrosis, stipple, or fleck. Foliar injury develops differently depending on plant species, genetic varieties, and age. Current ambient levels of ozone are reported to be high enough to cause chronic damage such as reduced photosynthesis and premature senescence, ultimately impairing plant growth, reducing crop yields and altering genetic composition of native plant communities (Darrall, 1989; Davison and Barnes, 1998; Runeckles and Chevone, 1992; Langebartels *et al.*, 1997). Decreased photosynthesis in trees due to long-term ozone exposure can contribute to forest decline.

The depression in net photosynthesis caused by ozone has been attributed to both limitation in stomatal conductance and to changes in mesophyll activity involved with CO₂ fixation (Farage and Long, 1999). Ozone causes significant changes in the primary photosynthetic reactions. A major effect of ozone includes a lowered PSII quantum yield which reflects a correspondingly reduced PSII electron transport rate and reduced CO₂ assimilation as well (Shavin *et al.*, 1999). Ozone is taken into the leaf via the stomata (Kerstiens and Lenzian, 1989) where it interacts with apoplastic components as well as the plasma membrane, and alters physiological function.

Membranes are the primary site of ozone interaction due to the susceptibility of membrane-bound molecules to ozone. It has been suggested that once ozone enters the leaf by diffusion through stomata, it is rapidly decomposed by a series of reactions in the cell walls and plasma membrane, leading to the production of reactive oxygen species, such as hydroxyl, peroxy, and superoxide radicals (Heath, 1994; Pellinen *et al.*, 1999; Langebartels *et al.*, 2002). However, it is still unclear whether the effects of ozone on net photosynthesis are based on direct oxidative damage within the chloroplast, or are a result of a signal produced from outside the chloroplast (Kangasjärvi *et al.*, 1994; Torsethaugen *et al.*, 1997; Wohlgemuth *et al.*, 2002). Ozone can also induce subtle physiological and biological changes that alter plant responses to a range of other biotic and abiotic stresses (Foyer *et al.*, 1994; Wellburn, 1997). Those changes may be as important as the direct effects of ozone.

Even though ozone is an anthropogenic air pollutant formed in urban and industrial areas, it has been reported to affect agricultural crop yield and to cause reductions in growth and biomass of forest tree species in remote and mountainous areas due to long-distance transport (Skelly, 2000). Many studies have investigated the impacts of tropospheric ozone on crop species. Research has focused on the relationship between ozone exposure and crop yield in order to assess the impact of current and predicted ambient ozone concentrations on agriculture (Bobbink *et al.*, 1998). Current ambient ozone concentrations are high enough to reduce yield in major agricultural crops, and as predicted levels are likely to increase, the loss to agriculture will be greater. According to Van der Eerden *et al.* (1988), the production of important crops, particularly wheat and soybeans, is reduced substantially, and crop losses of 5-10% have been estimated. An extensive investigation of crop loss due to ambient ozone with 15

major annual crops, including corn, soybean, cotton, forage, tomato, turnip, wheat, and barley, revealed yield depressions in 14 out of 15 crops studied. Losses attributed to ozone ranged from less than 1% in barley to as much as 20% in soybean (Lesser *et al.*, 1990).

Susceptibility to ozone varies from species to species, and even among cultivars of a single species. Comparison between sensitive and tolerant cultivars has been used for 30 years to assess ozone damage and to investigate the possible mechanisms (Rowland-Bamford *et al.*, 1989; Antonielli *et al.*, 1997). Several defense mechanisms have been suggested. Some studies showed stomata closure, avoiding ozone uptake. Other studies reported ozone-induced antioxidant defense systems (Schmieden *et al.*, 1993; D'Haese *et al.*, 2005). Several mechanisms that may be responsible for ozone tolerance have been put forth. Lower stomatal conductance of tolerant species results in a reduction in ozone uptake, and an increase in respiration rate and/or in antioxidants may help prevent and/or repair ozone damages (Degl'Innocenti *et al.*, 2002).

The tobacco cultivars Bel-W3 (sensitive) and Bel-B (tolerant) are widely known for their differential response to ozone, mostly due to differences in stomatal conductance, intercellular leaf volume, and soluble sugar or ascorbate content (Reiling and Davison, 1994; Ribas *et al.*, 1998, Degl'Innocenti *et al.*, 2002). Most studies examining ozone sensitivity and tolerance have focused on observing visible injury differentially represented by cultivars. A few studies have reported on the relation between inhibition of photosynthesis caused by ozone and its direct effect on stomatal closure and/or on changes in photosynthetic capacity at the mesophyll level (Loreto *et al.*, 1994; Degl'Innocenti *et al.*, 2002).

Bel-W3 has been used as an indicator of ozone for decades since it is extremely

sensitive to ozone. This cultivar develops easily recognizable visible symptoms. Bel-B is relatively ozone tolerant and it is often used with Bel-W3 to compare ozone-induced damage. Menser *et al.* (1966) reported that only 2 to 3 hours exposure to 0.05 to 0.06 ppm of ozone was enough to cause visible symptoms in Bel-W3. Ozone -induced foliar injury on Bel-W3 consists of bifacial necrosis; however, in Bel-B ozone-induced damage is typically upper surface flecking (Krupa *et al.*, 1993). Leaf injury increases linearly with increasing ozone concentration in Bel-W3 (Ribas *et al.*, 1998). The sensitivity to ozone increases as relative humidity and growth temperature increases. These environmental conditions affecting ozone sensitivity are closely related to stomatal behavior.

Degl'Innocenti *et al.* (2002) attempted to characterize photosynthetic response to a single fumigation of 150 ppm of ozone for 5 hours in Bel-B and Bel-W3 using chlorophyll fluorescence. In Bel-W3, not only were gas exchange parameters, photosynthetic rate and quantum yield for CO₂ assimilation reduced, but also chlorophyll fluorescence parameters including PSII efficiency. Bel-B showed ozone-induced reductions in only some chlorophyll fluorescence parameters, but recovered in 24 hours.

Ambient ozone concentrations have been reported to affect individual tree growth in forests as well. However, there is considerable variability in growth responses depending on plant age, species, and genotype sensitivity (Runeckles and Krupa, 1994). Because of the ubiquitous character of ozone and the fact that tree response can be altered by many other environmental factors, it is difficult to determine whether ambient ozone concentrations affect tree growth and forest productivity significantly (Chappelka and Samuelson, 1998; Vollenweider *et al.*, 2003). The general symptom induced by

ozone is visible foliar injury. Injury is generally distinguished as either acute or chronic responses. Acute foliar injury typically involves cell death and may be expressed as bifacial flecking with brown colored spots. Chronic injury generally develops on sensitive plant species as upper leaf surface pigmentation or stippling, premature leaf senescence and early leaf fall (Skelly, 2000). Several studies have attempted to define the relationship between visible ozone symptoms and growth losses. However, ozone-exposure/tree-response relationships have not been established clearly since ozone sensitivity is affected by species, tree developmental stage, microclimate, and the ability to compensate for injury through enhanced leaf production, and alteration in carbon partitioning and allocation (Chappelka and Samuelson, 1998; Skarby *et al.*, 1998).

Some species are known to be sensitive to ambient ozone concentrations. Such species are of particular interest in areas where air quality monitoring systems are not available. Using these sensitive species as bioindicators can assist in determining presence of ozone in a given area (Yuska *et al.*, 2003). Although the ozone sensitivity of native tree species has not been well established, the following trees are known to be relatively sensitive in northeastern forests in the United States: black cherry (*Prunus serotina* Ehrh.), white ash (*Fraxinus americana* L.), yellow poplar (*Liriodendron tulipifera* L.), and sassafras (*Sassafras albidum* Nees.) (Loats and Rebbeck, 1999; Orendovici *et al.*, 2003).

Black cherry is an economically important species in the eastern forest of the United States (Rebbeck, 1996). Black cherry has been well documented as one of the most ozone-sensitive trees in terms of expression of very distinctive foliar injury in the presence of elevated ambient ozone exposure (Neufeld *et al.*, 1995; Skelly *et al.*, 1997; VanderHeyden *et al.*, 2001). Symptoms are manifested as an upper leaf surface stipple

that appears in the mid to late growing season. Palisade cells in the leaf mesophyll are particularly sensitive to ozone injury and the collapse of individual cells or group of these cells produces visible symptoms on the leaf surface (Fredericksen *et al.*, 1996). Older leaves are more severely affected with advancing symptoms of premature senescence and defoliation (Skelly *et al.*, 1998). In field surveys, foliar injury, such as black, red, and purple stipple, on black cherry has been observed. Symptoms increased with increasing elevation and with increasing ozone concentration (Hilderbrand *et al.*, 1996; Clark *et al.*, 2000). With expression of apparent visible injury, black cherry has been considered as a potential bioindicator species of moderate ambient ozone levels (Davis and Skelly, 1992; Chappelka *et al.*, 1997; Bussotti *et al.*, 2003).

Physiological sensitivity to ambient ozone concentration has been examined. Samuelson (1994) found 2X ambient concentrations of ozone reduced net photosynthetic rate in both young and old leaves of shade grown black cherry seedlings by 23% but no effects of 1X ambient concentrations on net photosynthetic rate were observed. Rakonczay (1997) also observed that net photosynthetic rate was reduced up to 50% by 2X ambient concentrations of ozone in older leaves and root/shoot ratio also declined by 2X ambient concentrations of ozone, but no effects of 1X ambient concentrations of ozone on net photosynthetic rate and biomass were observed.

The development of instrumentation for the field measurements of modulated chlorophyll fluorescence has allowed the identification, separation, and quantification of chlorophyll fluorescence emitted from PSII directly (Schreiber *et al.*, 1986; Daley, 1995). Light energy absorbed by chlorophyll has to be dissipated in one of three ways: it can be used to drive photosynthesis (photochemistry), excess energy can be dissipated as heat, or it can be re-emitted as chlorophyll fluorescence (Peterson, 1989; Nielsen and

Orcutt, 1996). These three processes are competitive, so that any increase in the efficiency of one will result in a decrease in the yield of the other two (Schreiber *et al.*, 1986; Rohacek and Bartak, 1999). The usefulness of chlorophyll fluorescence from intact plant leaves has increased the ability to monitor photosynthetic events and characterize the physiological status of plants (Laisk and Walker, 1989; Scheidegger and Schroeter, 1995). As a result, measuring chlorophyll fluorescence has become a very attractive means of obtaining rapid, quantitative information on photosynthesis used by an increasing number of researchers. However, only limited studies have utilized chlorophyll fluorescence to understand the mechanisms involved in the ozone response of differentially susceptible cultivars at the photosynthetic level (Tausz *et al.*, 2004; Guidi *et al.*, 1997; Reiling and Davison, 1992).

The objectives of this research were to investigate effects of high ozone concentrations (200 ppb) on net CO₂ assimilation and PSII function in tobacco cultivars, Bel-B and Bel-W3, with different sensitivities to ozone and the effects of ambient atmospheric ozone concentrations on net CO₂ assimilation and PSII function in black cherry with different sensitivities to ozone under field conditions. Results from this research will contribute to a better understanding of the primary site of oxidative damage to the photosynthetic apparatus within the chloroplast and provide insights into the physiological mechanism of ozone toxicity.

Chapter 2

Ozone Alters CO₂ Exchange rates and Chlorophyll Fluorescence in Two Tobacco cultivars (*Nicotiana tabacum*) with different sensitivities

2.1 Introduction

Ozone (O₃) is formed by the photolysis of nitrogen dioxide (NO₂) via a series of complex photochemical reactions with both natural and anthropogenically derived gases. When atmospheric conditions are right, phytotoxic levels of ozone occur (Schraudner *et al.*, 1997; Saitanis and Karandinos, 2002). An increase in the production rate of ozone is consistent with precursor emissions and it is expected that the tropospheric ozone concentrations will continue to increase in the Northern Hemisphere (Chameides *et al.*, 1994). Ozone induces visible injury, reduces growth, decreases the rate of net photosynthesis, and accelerates foliar senescence in plants (Darrall, 1989; Runeckles and Chevone, 1992; Torsethaugen *et al.*, 1997; Davison and Barnes, 1998). Ozone enters the leaf through stomata and can react with membranes and other cell components causing leaf injury and impairing photosynthesis (Kerstiens and Lenzian, 1989; Runeckles and Chevone, 1992). Leaves which are expanding, or just fully expanded, are generally most susceptible, and the most severe ozone injury is usually found on older foliage (Ribas *et al.*, 1998).

Since the introduction of pulsed-fluorescence monitoring systems, chlorophyll fluorescence has been widely used to assess photosynthetic activity in plants (Schrieber *et al.*, 1986). The measurement of chlorophyll fluorescence is a non-invasive technique to assess the physiological state of the photosynthetic apparatus, not only indicating changes in overall photosynthetic capacity, but also allowing for localization of sites of damage (Genty *et al.*, 1990). The yield of chlorophyll fluorescence is determined by two distinct quenching

processes, photochemical (qP) and non-photochemical (qN) (Schreiber *et al.*, 1986). Photochemical quenching is proportional to the quantum yield of the linear electron transport rate and the efficiency of excitation capture by open photosystem II (PSII) reaction centers (Fv/Fm) under a wide range of physiological conditions. The rate of qN indicates regulatory adjustments in the photosynthetic membrane in response to altered external and internal conditions (Horton and Ruban, 1993).

Comparisons between sensitive and tolerant genotypes have been used for many years to assess ozone damage and to investigate sites of cellular injury (Antonielli *et al.*, 1997). Bel-W3 has been used as an indicator of ozone for decades since it is extremely sensitive to ozone and visible symptoms are easily recognizable (Heggstad, 1991). Bel-B, ozone-tolerant, is often used with Bel-W3 in indicator studies (Krupa *et al.* 1993). According to Heggstad (1991), ozone-induced foliar injury symptoms on Bel-W3 consist of upper surface flecking or bifacial necrosis, depending upon the severity of the ozone exposure. Under ambient ozone concentrations of 50 to 150 part per billion (ppb), Bel-B does not usually show foliar symptoms.

Although ozone-induced declines in photosynthesis have been well documented in numerous plant species (Pell *et al.*, 1994), the central question of where oxidative damage to the photosynthetic apparatus occurs has not yet been completely resolved (Torsethaugen *et al.*, 1997). This is true with the tobacco cultivars Bel-W3 and Bel-B, where surprisingly little information on photosynthetic function and gas exchange measures is available. In this present study, we examined whether a moderately high ozone concentration differentially affected net CO₂ fixation and PSII function in the cultivars Bel-W3 and Bel-B.

2.2 Materials and Methods

2.2.1 Plant material and growth conditions

Two varieties of tobacco (*Nicotiana tabacum L.*), Bel-W3 and Bel-B, were chosen because of their known differences in ozone sensitivity (Menser *et al.*, 1966). Germination and initial growth of plants took place in a greenhouse supplied with charcoal-filtered (CF) air to reduce ozone concentration below 25 ppb under a day temperature of 22-30°C. All plants were grown until the 7-8-leaf stage prior to ozone exposure in 10-cm diameter pots containing potting mixture Metromix 200[®].

2.2.2 Ozone exposure

Plants were exposed to 200 ppb of ozone or to CF air (containing less than 10 ppb ozone) for 4hr in CSTR (Continuously Stirred Tank Reactor) chambers in the greenhouse. Ozone was generated from oxygen by UV discharge and supplied to the chambers using rotometers. A TECO (Thermo Electron Corporation, Waltham, MA) ozone analyzer recorded ozone concentrations continuously and data were stored electronically. During the fumigation, plants were exposed to a light level of $1100 \pm 100 \mu\text{mol m}^{-2} \text{s}^{-1}$ PAR, temperatures of 25-30 °C, R.H. of 45-55% and 350 ppm CO₂.

2.2.3 Visible injury

The appearance of visible injury was evaluated 48 hr after fumigation was completed. The 3rd, 4th, and 5th leaves were rated on a scale from 0 to 100, corresponding to the percentage of visible injury covering the upper leaf surface.

2.2.4 Net photosynthesis

Gas exchange measurements were conducted using a Li-Cor Li-6400 portable photosynthesis system (LiCor, Lincoln, NE). Net photosynthesis under saturating light

conditions (Pn_{MAX} , $\mu\text{mol CO}_2 \text{ m}^{-2}\text{s}^{-1}$ at $900 \mu\text{mol m}^{-2}\text{s}^{-1}\text{PAR}$) and 350 ppm CO_2 , and stomatal conductance (g_s , $\text{mmol H}_2\text{O m}^{-2}\text{s}^{-1}$) were measured immediately after exposure and at 24 hr intervals for three days on the 4th leaf position (The first apical leaf that was at least 8 cm long was designated leaf one). Assimilation-irradiation curves were generated under ambient CO_2 concentrations. From the initial slope of these curves, the apparent quantum efficiency for net CO_2 assimilation (ΦCO_2) was determined.

2.2.5 Chlorophyll fluorescence

A PAM-2000 (Heinz Walz, Germany) portable, pulse-modulated fluorometer was used to measure chlorophyll fluorescence yield. Analysis of fluorescence characteristics was made on the adaxial surface of the same leaf tissue utilized for monitoring gas exchange rates immediately after ozone fumigation. Pulse frequency was 600 Hz for detection of minimal PSII fluorescence and 20,000 Hz for light induced fluorescence. Saturating light pulses, to reduce all PSII reaction centers, were at $10,000 \mu\text{mol m}^{-2}\text{s}^{-1}$. Leaves were dark adapted for a minimum of 15 minutes prior to determination of maximum (F_m) and minimum (F_o) fluorescence. Variable fluorescence ($F_v = F_m - F_o$), an indicator of the maximum quantum efficiency for photochemistry, was calculated according to Schreiber *et al.* (1986). For maximum photosynthetic activity, leaves were exposed to actinic illumination at $950 \pm 50 \mu\text{mol m}^{-2} \text{ s}^{-1}$ PAR for 20 minutes and a saturating flash of white light was given at 20-second intervals. A leaf clip holder (2030-B Heinz Walz, Germany) was used for monitoring PAR and leaf temperature during actinic illumination. Estimates of photochemical (q_P) and non-photochemical (q_N) quenching co-efficient were determined by the pulse saturation method and both quenching co-efficient q_P ($F'_m - F_s / F'_m - F'_o$) and q_N ($F_m - F'_m / F_m - F'_o$) were calculated where F_s represents steady state fluorescence. Quantum yield for linear electron transport through PSII, Φ_{PSII} ($\Delta F / F'_m$), was determined. The maximum electron transport rate was calculated according to Genty *et al.* (1990) at $950 \pm 50 \mu\text{mol m}^{-2}\text{s}^{-1}$ PAR using equation:

$$\text{ETR} = \Phi_{\text{PSII}} \times \text{PAR} \times 0.5 \times 0.84$$

where 0.5 corresponds to the two photosystems, 0.84 is an estimate of the fraction of incident PAR that is absorbed, and PAR is the value for the light intensity given

2.2.6 Experimental design and statistical analysis

One control and one ozone treated CSTR containing 3 plants of each cultivar were used for fumigation. Fumigations were repeated three times for a total of nine replicates for each cultivar and each treatment. Data were analyzed by analysis of variance with ozone treatments and cultivars as class variables. When significance is noted, it refers to statistical significance at $P \leq 0.05$ with a single asterisk and at $P \leq 0.01$ with two asterisks.

2.3 Results

2.3.1 Photosynthetic function in control plants

The rates of net CO₂ assimilation at the 4th leaf position of the two tobacco cultivars, Bel-W3 and Bel-B, exposed to charcoal-filtered (CF) air were similar at low light intensity. However, they began to diverge as light intensity exceeded 300 $\mu\text{mol m}^{-2}\text{s}^{-1}$ PAR (**Figure 2.1**). At saturating light intensity (900 $\mu\text{mol m}^{-2}\text{s}^{-1}$ PAR), the maximum net photosynthetic rate ($P_{n\text{MAX}}$) was about 8.5% higher in the tolerant cultivar, Bel-B (11.4 $\mu\text{mol CO}_2 \text{ m}^{-2}\text{s}^{-1}$), than in sensitive cultivar, Bel-W3 (10.5 $\mu\text{mol CO}_2 \text{ m}^{-2}\text{s}^{-1}$) (**Table 2.1**). The apparent quantum yield for CO₂ assimilation, Φ_{CO_2} , was very similar between the two cultivars at 0.055 and 0.054 $\mu\text{moles CO}_2 \mu\text{mol photon}^{-1}$ for Bel-B and Bel-W3, respectively (**Figure 2.1**, insert; **Table 2.2**). Stomatal conductance (g_s) was about 36% higher in Bel-B (225 $\text{mmol H}_2\text{O m}^{-2}\text{s}^{-1}$) than in Bel-W3 (165 $\text{mmol H}_2\text{O m}^{-2}\text{s}^{-1}$) at saturating light intensity (**Table 2.3**), indicating the

potential for greater initial ozone uptake into the leaf in the tolerant cultivar.

Since photosynthetic activity was measured over a 72-hr period after ozone fumigation, the effect of leaf age on physiological activity was measured for 17 days beginning when a leaf attained 8 cm in length. **Figure 2.2** shows the changes in the maximum rate of net CO₂ assimilation (**A**), stomatal conductance (**B**), and internal CO₂ concentration (**C**) in relation to leaf age in Bel-W3 and Bel-B. The time period designated by the arrows indicates the 6 to 8-leaf stage when plants were fumigated with ozone and photosynthetic function was measured. Maximum photosynthetic rates (Pn_{MAX}) were approximately 6 $\mu\text{mol CO}_2 \text{ m}^{-2} \text{ s}^{-1}$ in the 8 cm length leaf (day 1), reached a peak at 10 $\mu\text{mol CO}_2 \text{ m}^{-2} \text{ s}^{-1}$ on day 7 to 10, and then declined. Stomatal conductance (g_s) attained a maximum at about 3 days and then tended to decrease during the measuring period. The internal CO₂ (C_i) concentration, reflecting the net assimilation rate, was highest in young leaves, when photosynthesis was increasing, and lower in senescent leaves, when photosynthesis was declining. The time period designated by the arrows in **Figure 2.2**, corresponding to the 72-hr of ozone fumigation and monitoring of physiological activity, corresponded to the period of maximum photosynthesis and early senescence of the 4th leaf.

2.3.2 Visible foliar symptoms

The sensitive cultivar, Bel-W3, developed visible injury symptoms within 48 hr post fumigation on the 3rd, 4th and 5th leaves. Symptoms appeared as white, necrotic spots, principally on the upper leaf surface, confined to the tips and margins in young foliage, but covering the entire surface in older leaves. Visible injury was less prevalent in young foliage (20% at the 3rd leaf position) than older foliage (50% at the 5th leaf position) (**Figure 2.3A**). The tolerant cultivar, Bel-B was less symptomatic with only 5% of the total area affected on the most severely injured leaf (**Figure 2.3A**). **Figure 2.3B** shows the appearance of visible foliar injury on the 4th leaf comparing the sensitive cultivar Bel-W3 and tolerant cultivar Bel-

B.

2.3.3 Photosynthetic function in ozone-treated plants

Exposure to 200 ppb of ozone for 4hr caused an immediate depression in maximum photosynthetic rate (Pn_{MAX}) in both tolerant and sensitive cultivars (**Table 2.1**). The Pn_{MAX} of ozone-treated Bel-B was reduced 36% compared to control plants immediately after fumigation; however, CO_2 fixation recovered to near control rates within 24 hrs post fumigation and this recovery persisted through the 72-hr measuring period (**Table 2.1, Figure 2.4A**). On the other hand, ozone exposure reduced Pn_{MAX} up to 50%, with no recovery, in Bel-W3, apparently causing permanent damage to the photosystem (**Figure 2.4A**). The Pn_{MAX} in both control and fumigated plants gradually decreased as a function of the aging process (**Table 2.1**).

Apparent quantum yield for CO_2 fixation, Φ_{CO_2} , was affected by ozone fumigation in a pattern similar to maximum photosynthetic rates (**Table 2.2**). Reductions in Φ_{CO_2} calculated from the assimilation-irradiation response curves differed between tolerant and sensitive cultivars (**Figure 2.4B**). Bel-B showed an immediate depression of 14% compared to controls after fumigation, whereas Bel-W3 showed a 27% decline. Φ_{CO_2} began to recover in Bel-B within 24 hr, and by 48 hr-post fumigation, Φ_{CO_2} was similar to controls. However, no apparent trend towards recovery was evident in Bel-W3 (**Figure 2.4B**). Φ_{CO_2} in Bel-W3 was still 25% less than in the controls at 72 hours after fumigation.

Stomatal conductance, g_s , also decreased after ozone fumigation in both cultivars (**Table 2.3**). In Bel-B and Bel-W3, g_s was 48% lower than in the controls immediately after fumigation, but recovered within 24 hr post fumigation in the tolerant cultivar. In Bel-W3, recovery was less apparent, and g_s was still 39% lower than in control plants 72 hr post ozone fumigation ended.

Figure 2.1 Net assimilation ($\mu\text{mol CO}_2 \text{ m}^{-2}\text{s}^{-1}$) - irradiance (PAR; $\mu\text{mol m}^{-2}\text{s}^{-1}$) on the 4th leaf position of control tobacco plants, Bel-B (BBC; open circles) and Bel-W3 (BWC; closed squares). Insert shows the initial slopes of the A-I response curves. Bars represent \pm one standard deviation and, where not apparent, are contained within the symbols.

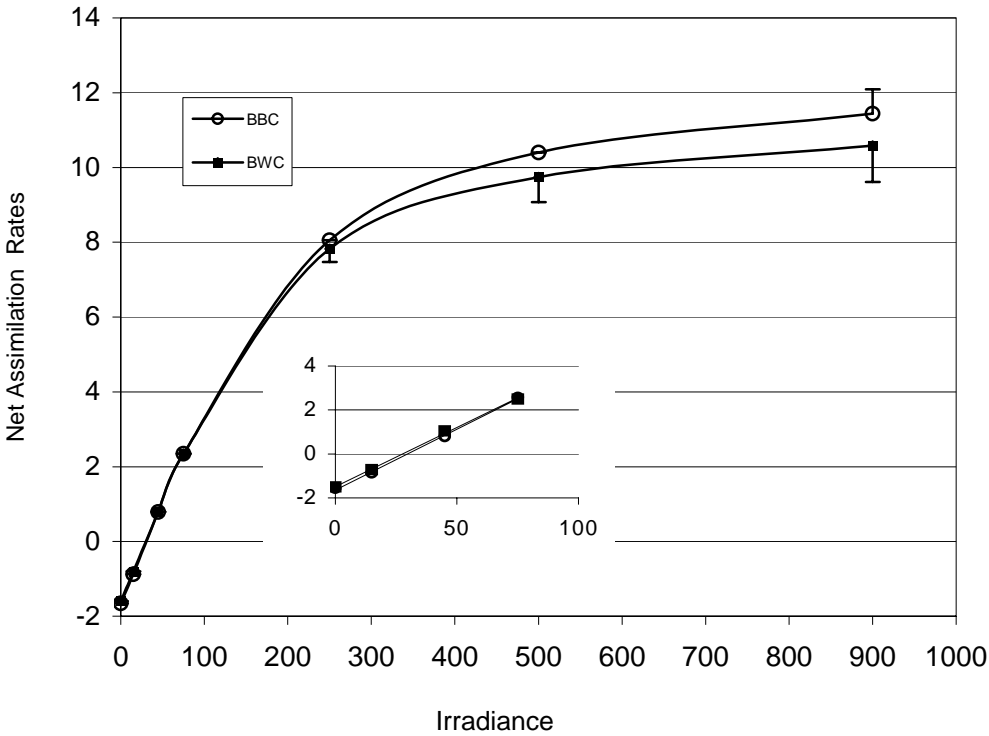


Figure 2.2 (A) Maximum net photosynthetic rate (Pn_{MAX} , $\mu\text{mol CO}_2 \text{ m}^{-2}\text{s}^{-1}$) (B) stomatal conductance (g_s , $\text{mmol H}_2\text{O m}^{-2}\text{s}^{-1}$), and (C) internal CO_2 concentration (C_i , ppm) in relation to leaf age in Bel-B (closed circles) and Bel-W3 (closed squares) (leaf 8 cm long at day 1) in non-fumigated plants. Arrow indicates the ozone fumigation and block indicates duration of experimental period. Bars represent \pm one standard deviation and, where not apparent, are contained within the symbols. Lines were fitted by polynomial (A) and linear (B) and (C) regression.

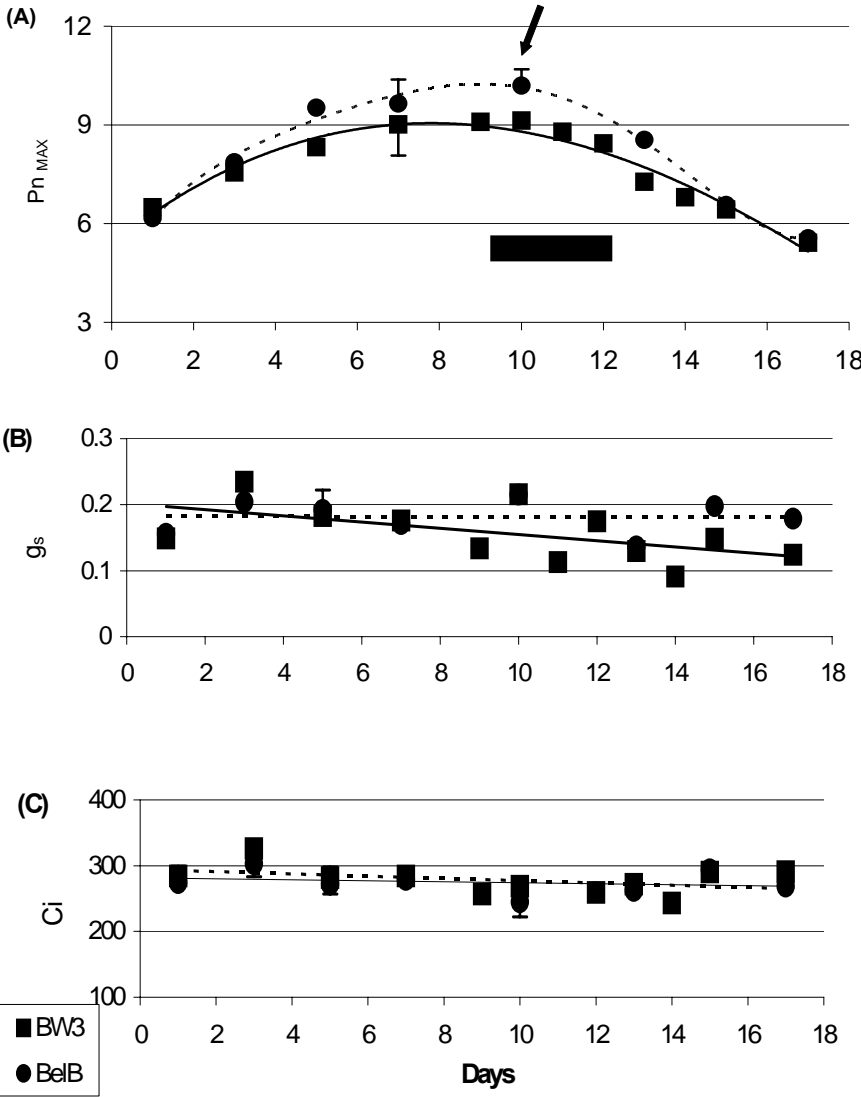


Table 2.1 Maximum net photosynthetic rates (Pn_{MAX} , $\mu\text{mol CO}_2 \text{ m}^{-2} \text{ s}^{-1}$ at $900 \mu\text{mol m}^{-2}\text{s}^{-1}$) in Bel-B (tolerant) and Bel-W3 (sensitive) tobacco cultivars after exposure to 200 ppb ozone for 4 hr. Single asterisk indicates significant differences from control plants at $P < 0.05$. Values are means \pm s.d.

Cultivar	Treatment	<i>Time post-O₃-fumigation (h)</i>			
		<i>0</i>	<i>24</i>	<i>48</i>	<i>72</i>
Bel-B	Control	11.35 \pm 0.33	10.95 \pm 0.69	10.23 \pm 0.48	8.03 \pm 0.28
	O ₃	7.28 \pm 0.33*	11.23 \pm 0.13	9.76 \pm 0.50	7.31 \pm 0.10
Bel-W3	Control	10.46 \pm 0.82	11.5 \pm 0.48	10.24 \pm 1.24	8.99 \pm 0.69
	O ₃	6.06 \pm 0.32*	5.83 \pm 0.68*	7.08 \pm 0.24*	5.84 \pm 0.61*

Table 2.2 Quantum yield for CO₂ assimilation ($\mu\text{mol CO}_2 \mu\text{mol photons}^{-1}$) in Bel-B and Bel-W3 tobacco cultivars after exposure to 200 ppb ozone for 4 hr. Single asterisk indicates significant differences from control plants at $P < 0.05$, two asterisks indicate significant differences at $P < 0.01$. Values are means \pm s.d.

Cultivar	treatment	Time post-fumigation (h)			
		0	24	48	72
Bel-B	Control	0.055 \pm 0.001	0.051 \pm 0.004	0.049 \pm 0.001	0.049 \pm 0.002
	O ₃	0.048 \pm 0.005**	0.047 \pm 0.004	0.048 \pm 0.001	0.048 \pm 0.003
Bel-W3	Control	0.054 \pm 0.002	0.050 \pm 0.003	0.049 \pm 0.005	0.049 \pm 0.005
	O ₃	0.039 \pm 0.007**	0.041 \pm 0.006**	0.037 \pm 0.002*	0.042 \pm 0.004*

Table 2.3 Stomatal conductance (g_{ss} , $\text{mmol H}_2\text{O m}^{-2}\text{s}^{-1}$) in Bel-B and Bel-W3 tobacco cultivars after exposure to 200 ppb ozone for 4 hr. Single asterisk indicates significant differences from control plants at $P < 0.05$. Values are means \pm s.d.

Cultivar	Treatment	Time post-fumigation (h)			
		0	24	48	72
Bel-B	Control	0.225 \pm 0.053	0.250 \pm 0.072	0.212 \pm 0.036	0.148 \pm 0.046
	O ₃	0.116 \pm 0.057*	0.230 \pm 0.028	0.175 \pm 0.007	0.157 \pm 0.046
Bel-W3	Control	0.165 \pm 0.040	0.218 \pm 0.042	0.176 \pm 0.024	0.178 \pm 0.652
	O ₃	0.086 \pm 0.042*	0.142 \pm 0.050*	0.104 \pm 0.028**	0.108 \pm 0.024*

Figure 2.3 Visible symptoms on the foliage 48 hr post-ozone-fumigation (200 ppb for 4 hr) in tobacco cultivars Bel-B (black bars) and Bel-W3 (white bars), (A) percentage of visible injury and (B) appearance of foliar injury on the 4th leaf position.

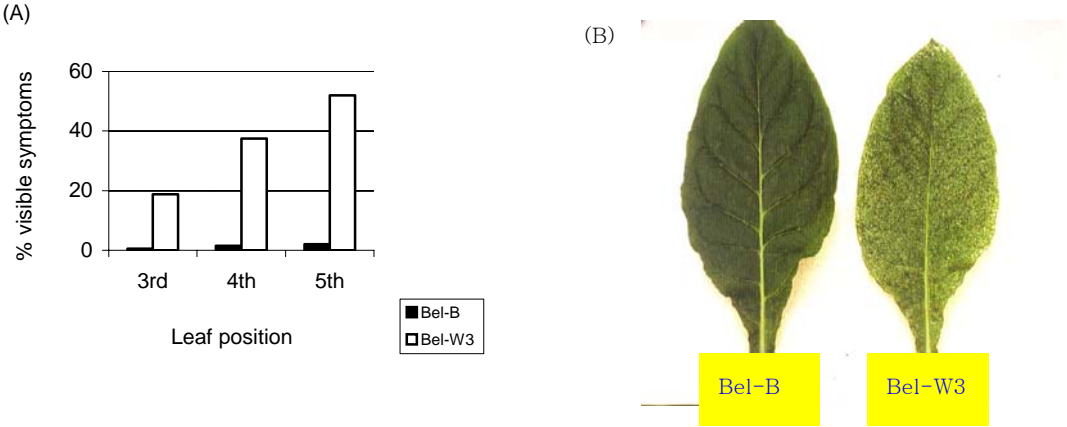
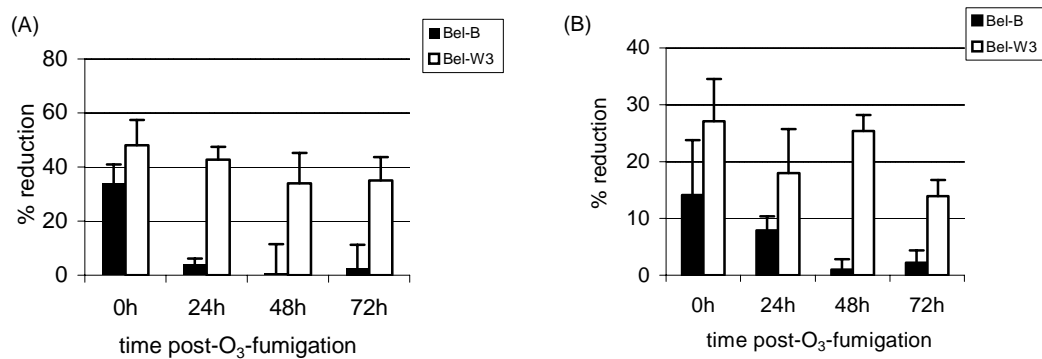


Figure 2.4 (A) Percentage reduction of maximum net photosynthetic rates and (B) percentage reduction of quantum yield for CO₂ assimilation in Bel-B (black bars) and Bel-W3 (white bars) tobacco cultivars exposed to 200 ppb of ozone for 4 hr. Initial rates are taken from control plants at 0 hr post-ozone-fumigation. Bars represent one standard deviation.



2.3.4 Chlorophyll fluorescence in control and ozone-treated plants

Photochemical efficiency (F_v/F_m), measured in the dark-adapted state immediately after fumigation, decreased 7% and 18% in Bel-B and Bel-W3, respectively (**Figure 2.5**). However, the contributions to the decreased ratio of F_v/F_m were different between cultivars. The maximum level of chlorophyll fluorescence (F_m) decreased more in Bel-W3 than Bel-B, whereas minimum fluorescence (F_o) increased more in Bel-B than Bel-W3 (**Figure 2.6**). Electron transport rates (ETR) in both cultivars decreased at all irradiance levels immediately after ozone exposure. At saturating light intensity, ETR decreased 58% and 80% in Bel-B and Bel-W3, respectively (**Figure 2.6A**). The quantum yield for transporting electrons from PSII, Φ_{PSII} , measured by the chlorophyll fluorescence method, decreased immediately post-fumigation by 28% and 36% in Bel-B and Bel-W3, respectively (**Figure 2.6B**).

2.4 Discussion

2.4.1 Effects of high concentration of ozone on tobacco

The decrease in Pn_{MAX} was greater in the sensitive cultivar, Bel-W3, than in the tolerant cultivar Bel-B. The decline in Pn_{MAX} in Bel-W3 appears due to permanent damage in the PSII reaction center which results in more than a 2X drop in F_v/F_m ratio with a substantial reduction in F_m . The increase of F_o may also be responsible for this reduction of the F_v/F_m ratio in Bel-W3. The fact that the maximum fluorescence level (F_m) was suppressed before any effect on the initial level (F_o) occurred showed that initial damage to the PSII donor site took place prior to any decrease in energy transfer efficiency within the pigment system.

However, the response of the tolerant cultivar was different. Bel-B also showed a decrease in the F_v/F_m ratio after ozone exposure which was mostly due to an increase in F_o with unchanged F_m .

Figure 2.5 Percentage difference in dark adapted state chlorophyll fluorescence parameters F_o minimum chlorophyll fluorescence (black bars) F_m maximum chlorophyll fluorescence (grey bars) and $F_v[F_m-F_o]/F_m$ maximum photochemical efficiency of PSII (white bars) in Bel-B and Bel-W3 tobacco cultivars immediately after ozone fumigation of 200 ppb ozone for 4 hr. Bars represent one standard deviation.

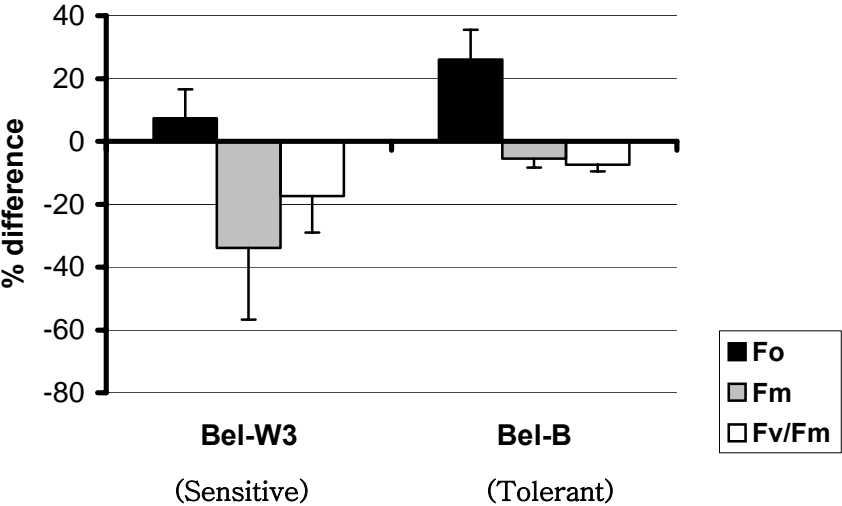


Figure 2.6 (A) electron transport rates of PSII (ETR, $\mu\text{mol electron m}^{-2}\text{s}^{-1}$) and (B) quantum efficiency for PSII (Φ_{PSII}) – Irradiance (PAR $\mu\text{mol m}^{-2}\text{s}^{-1}$) response curves on the 4th leaf in Bel-B (BBC, control plants and BBO, ozone treated plants) and Bel-W3 (BWC, control plants and BWO, ozone treated plants) tobacco cultivars immediately after ozone fumigation with 200 ppb of ozone for 4hr. Bars represent \pm one standard deviation.

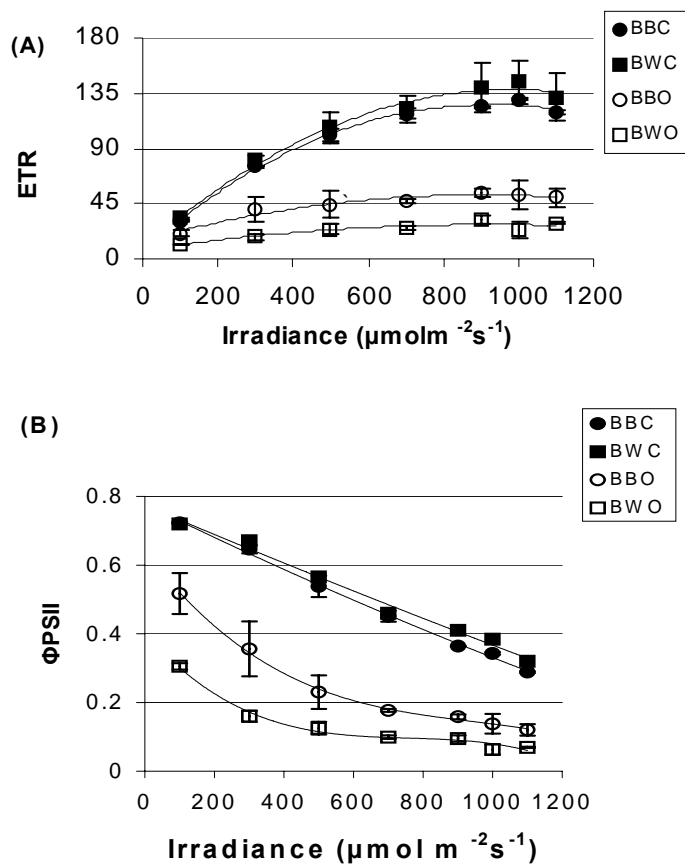


Table 2.4 Fluorescence characteristics and the apparent electron transport rate (ETR) in leaves of Bel-B and Bel-W3 immediately after ozone fumigation at 200 ppb for 4hr. Asterisks indicate significant differences from control plants at P<0.05. Values are mean \pm s.d.

Parameters	<i>Bel-B</i>		<i>Bel-W3</i>	
	<i>Control</i>	<i>O₃</i>	<i>Control</i>	<i>O₃</i>
Fm	1.916 \pm 0.026	1.810 \pm 0.031*	1.952 \pm 0.043	1.258 \pm 0.396*
Fo	0.348 \pm 0.017	0.439 \pm 0.015*	0.353 \pm 0.004	0.388 \pm 0.024*
Fv	1.568 \pm 0.036	1.371 \pm 0.031*	1.598 \pm 0.044	0.870 \pm 0.415*
Fv/Fm	0.818 \pm 0.010	0.758 \pm 0.009*	0.819 \pm 0.004	0.670 \pm 0.105*
ϕ_{PSII}	0.364 \pm 0.001	0.158 \pm 0.007	0.41 \pm 0.052	0.102 \pm 0.012
ETR	123 \pm 6.0	54 \pm 3.0*	139 \pm 19.8	33 \pm 3.5*
qP	0.449 \pm 0.011	0.215 \pm 0.060	0.495 \pm 0.062	0.191 \pm 0.001
qN	0.578 \pm 0.046	0.463 \pm 0.040	0.560 \pm 0.135	0.615 \pm 0.008

Table 2. 5. Summary of photosynthetic activities, gas exchange and chlorophyll fluorescence, before and after ozone fumigation in tobacco cultivars. Prior to ozone fumigation percentage reduction calculated as $(T-S)/T \times 100$ (T, tolerant; S, sensitive). With ozone fumigation, percentage reduction calculated as $(C-O)/C \times 100$ (C, control plants; O, ozone treated plants)

	<i>Tolerant</i>	<i>Sensitive</i>
	Bel-B	Bel-W3
Before fumigation		
with O₃		
Pn _{MAX}	8.5 % higher	
ΦCO ₂	Same	Same
g _s	36% higher	
After fumigation		
with O₃		
Visible Symptoms	Less than 5%	20% to 50% depending on leaf position
Pn _{MAX}	Immediate reduction of 36%	Immediate reduction of 50%
ΦCO ₂	Immediate reduction of 14%	Immediate reduction of 27%
g _s	Immediate reduction of 48%	Immediate reduction of 61%
Fv/Fm	Immediate reduction of 7% Mostly due to increased Fo	Immediate reduction of 18% Mostly due to decreased Fm with minimum increased Fo
Φ _{PSII}	Immediate reduction of 28%	Immediate reduction of 36%
ETR	Immediate reduction of 58%	Immediate reduction of 80%
Recovery	Within 24 hr of post fumigation	No recovery, Permanent damage

The decrease in the Fv/Fm ratio may be associated with photoinhibitory damage indicating an altered electron transport rate of PSII to PSI by the increasing Fo. The maximum photochemical efficiency (Φ_{PSII}) was reduced dramatically in both cultivars. This was due to the decrease in qP and consequently an increase in the 1-qP parameter. The decrease in Φ_{PSII} was greater in the sensitive cultivar. According to Van Buuren *et al.* (2002), 1-qP can be a measure of the reduction state of the primary quinone acceptor. In this instance, an increase in 1-qP indicates a less effective re-oxidation of this electron acceptor, suggesting in turn that some fraction of the PSII traps were closed during actinic illumination. These closed traps lead to decreased quantum efficiency of PSII.

The apparent quantum yield also decreased to a greater extent in the sensitive cultivar compared to the tolerant one. However, the concentration of ozone used in this fumigation study may have been sufficiently high that not only did visible injury symptoms develop, but photosynthetic activity decreased in the tolerant cultivar. Gupta *et al.* (1991) found that a reduction in CO₂ fixation was least sensitive to ozone, and the decline in photosynthesis may be a secondary effect due to less reductant being available for carbon reduction. If CO₂ fixation cannot keep pace with NADPH production, the NADP pools become reduced with an excess reduction of PSII and PSI. Under these conditions, O₂ can compete for electrons from PSI leading to the generation of reactive oxygen intermediates through the Mehler reaction (Allen, 1995). The increases in the non-photochemical quenching coefficient of fluorescence, qN, also dissipates extra absorbed energy, that not consumed by carbon metabolism, as heat and prevents over-reduction of the electron transport chain (Habash *et al.*, 1996). Mechanisms of qN are still unknown; however, many of its characteristics are generally

accepted. One of them is the xanthophylls cycle, converting violaxanthin to zeaxanthin via the intermediate of antheraxanthin through increasing the trans-thylakoid pH gradient and activating the high light-triggered violaxanthin de-epoxidase enzyme (Dall'Osto *et al.*, 2005). The lower assimilation rate was reflected in the reduction in photochemical quenching, qP, which is an estimate of the number of open or oxidized PSII centers. The difference between total linear electron transport and electrons being used for carbon assimilation may indicate the existence of alternative electron sinks such as photorespiration, Mehler reaction, and nitrite reduction (Habash *et al.*, 1996).

Ozone causes nonspecific changes in fluorescence parameters. The effects of ozone on whole plants can be determined with the chlorophyll fluorescence induction assay. In 1978, Schreiber *et al.* reported that the way in which fluorescence induction is affected may suggest the sites of ozone damage within the photosynthetic apparatus. The fact that the initial level (F_o) is suppressed before any effect on the maximum level (F_m) occurs indicates initial damage to the PSII donor site prior to any decrease in energy transfer efficiency within the pigment system. The electron transport from PSII to PSI also becomes inhibited as indicated by increasing F_o.

In summary, in both cultivars, along with decreased maximum net photosynthesis and stomatal conductance, quantum yield for CO₂ fixation decreased immediately following ozone fumigation. Maximum electron transport rate through PSII to PSI and quantum yield of PSII decrease in both cultivars immediately following ozone fumigation. Fumigation at 200 ppb concentration for 4 hr was severe enough to cause reductions in physiological function in Bel-B, the tolerant cultivar. Ozone caused a greater relative decrease in linear electron transport than maximum net photosynthesis, suggesting greater damage to PSII than the carbon reduction cycle in the sensitive

cultivar. Physiological functions in the tolerant cultivar were only temporarily impaired, and recovered fully by 24 hr-post-fumigation. However, the damage caused by the high concentration of ozone in the sensitive cultivar was permanent and no recovery was observed.

Chapter 3

Photosynthetic response of tolerant and sensitive black cherry (*Prunus serotina*) to ambient ozone concentrations under natural conditions

3.1 Introduction

The most widespread and phytotoxic air pollutant impacting forests in the eastern United States is the oxidant ozone (USEPA, 1996). During the summer months, rural ozone concentrations are sufficiently high to cause visible foliar symptoms on a number of tree species including white and green ash, hickory, yellow poplar, black cherry and eastern white pine (Loats and Rebbeck, 1999; Orendovici *et al.*, 2003). Black cherry (*Prunus serotina* Ehrh.) is a significant component of the eastern forests (Rebbeck, 1996) and is one of the most ozone-sensitive hardwoods based on the appearance of leaf injury (Davis *et al.*, 1977; Simini *et al.*, 1992; Hildebrand *et al.*, 1996). In a regional assessment of ozone-sensitive tree species in the northeastern and mid-Atlantic areas, black cherry was placed in the highest risk category (Coulston *et al.*, 2003). Trees located in the Allegheny Mountains of West Virginia, central Pennsylvania and the Delmarva eastern shore were at greatest risk with an estimated biosite site index (injury incidence x severity) greater than 20. Trees growing in the Blacksburg, VA area were at moderate risk with a biosite index of 15 to 20.

Considerable diversity in symptom expression occurs within black cherry and this variation in oxidant response has been demonstrated in wild populations as well as clonal lines and half-sib families (Fredericksen *et al.*, 1996; Kouterick *et al.*, 2000; Lee *et al.*, 2002). The effect of ozone on leaf symptom development and leaf senescence has been studied quite extensively in both open-top chambers and under natural field

conditions (Skelly *et al.*, 1998; VanderHeyden *et al.*, 2001). Foliar symptom expression is affected by genotype, tree age, leaf age, crown position, light intensity, tree water status, stomatal conductance and leaf morphology (Fredericksen *et al.*, 1996; Chappelka and Samuelson, 1998; Schraudner *et al.*, 1997; Ferdinand *et al.*, 2000; Schaub *et al.*, 2003; Schaub *et al.*, 2005). However, the relationship between foliar injury and net carbon assimilation is less well characterized. This is especially true for black cherry growing in their natural environment and is primarily attributed to a lack of adequate controls (Coulston *et al.*, 2003; Bennett *et al.*, 2006). In central Massachusetts, stem diameter of sensitive trees was reduced by 28% compared to asymptomatic trees over a 31-year period (Vollenweider *et al.*, 2003), and at southern Lake Michigan, greater foliar injury was associated with an 18% decrease in branch elongation (Bennett *et al.*, 2006). These observations suggest that differences in carbon fixation between sensitive and tolerant phenotypes, associated with foliar injury, may be responsible for the variation in growth and biomass accumulation.

Foliar injury and leaf gas exchange rates have been measured in black cherry seedlings in controlled environments and open-top chambers and in field-grown mature trees with mixed results. In most cases, no differences in net carbon uptake were observed between symptomatic and non-injured leaves (Schaub *et al.*, 2003; Schaub *et al.*, 2005). In a controlled environment, one-year-old seedlings demonstrated foliar injury at 2X ambient ozone concentrations and a weak trend toward reduced net photosynthesis as symptoms increased (Samuelson, 1994). In the only study comparing tolerant and sensitive phenotypes, half-sib, sensitive, one-year-old seedlings had higher net photosynthetic rates and greater leaf injury than tolerant seedlings (Kouterick *et al.*, 2000).

Because of the discrepancies in the literature relating foliar injury to net carbon assimilation, the present study was conducted to establish the relationship between foliar injury and photosynthetic function using ozone-tolerant and sensitive black cherry trees growing under natural conditions. Gas exchange rates, leaf injury, and incident radiation/CO₂ net assimilation curves were determined on a specific leaf position throughout the growing season to characterize the effects of cumulative ozone exposure on physiological leaf injury. The study was conducted over three years at three different sites to assess the consistency of leaf response to ambient ozone concentrations and environmental conditions.

3.2 Materials and Methods

3.2.1 Experimental site and design

This study was conducted for three consecutive years, 2000, 2001, and 2002 during the growing season from May to September. The sites were selected in the vicinity of an Air Quality Monitoring Station located at the Horton Research Center in Giles County, VA. A TECO ozone analyzer (Thermo Electron Corporation, Waltham, MA) was used to measure ambient ozone concentrations. Ozone data were collected during the growing season each year. Cumulative ozone exposures (SUM00 and SUM40) were calculated by summing the daily hourly averages (0700 to 1900 h) from May 2 to September 15. SUM00 values were calculated with 0 ppb as the base, whereas SUM40 values were the sum of those concentrations ≥ 40 ppb (based on Lee *et al.*, 1988).

Two groups of black cherry with contrasting sensitivities to ozone were selected. The sensitivity was deduced from the severity of foliar symptoms, occurring as upper

leaf flecking and dead tissue, observed during the previous summer. Three replicate trees of each ozone sensitivity class (sensitive or tolerant) were selected. Each experimental unit consisted of two branches from a single tree; readings from the 3rd leaf position on each branch were averaged. Three experimental sites were selected within 15 miles of the Air Quality Monitoring Station: the edge of Blacksburg at Mountain Tabor Rd., VA (MTB), the Air Pollution Lab at Virginia Tech which is located near downtown Blacksburg (APL), and the Horton Research Center with the Air Quality Monitoring facility in Giles County (HRC). Comprehensive measurements were made at HRC in all three years; supplemental data were collected at MTB in 2000, and at APL in 2001 and 2002. Three mature trees were selected with similar size at 4-5m tall, in each sensitivity class. Trees grew at the edge of a pasture or field and situated within 25m of each other. During the growing season of each year, monthly gas exchange and chlorophyll fluorescence measurements were performed on the 3rd basal leaf from the mid crown facing east.

3.2.2 Foliar visible injury and chlorophyll content

Visible injury was evaluated at two-week intervals beginning in mid-May until the end of the season in mid-September each year. Throughout the summer, leaf positions two through six (counting from the base) were rated from 0 to 100, corresponding to the percentage of visible injury occurring on the upper leaf surface.

Leaf discs 0.7 cm in diameter were sampled to determine total chlorophyll concentrations. Extraction was performed with 5 ml of DMSO solvent. Concentrations of chlorophyll a and b were determined spectrophotometrically at wavelengths of 663 nm and 645 nm, respectively, according to Barnes *et al.* (1992). Monthly during each

growing season from June to August, total chlorophyll concentrations on the 3rd leaves were compared between sensitive and tolerant black cherry. In September, the relationship between total chlorophyll concentrations and percentage leaf injury was evaluated for sensitive trees.

3.2.3 Net photosynthesis

Leaf gas exchange analysis was conducted with a Li-Cor 6400 portable photosynthesis system with 2X3 cm cuvette with a blue–red LED light source (Li-Cor Inc., Lincoln, NE). Maximum net photosynthetic rate, net photosynthetic rate under saturating light conditions (Pn_{MAX} , $\mu\text{mol CO}_2 \text{ m}^{-2}\text{s}^{-1}$ at $900 \mu\text{mol m}^{-2}\text{s}^{-1}$ PAR and 350 ppm CO_2) and stomatal conductance (g_s , $\text{mol H}_2\text{O m}^{-2}\text{s}^{-1}$) were determined monthly on the 3rd leaf at HRC in each year. At MTB and APL, supplementary early and late season data were obtained in 2000 through 2002. Assimilation–irradiance response curves (A-I) were obtained by measuring Pn at 350 ppm CO_2 concentration and irradiance ranging from 0 to $1800 \mu\text{mol m}^{-2}\text{s}^{-1}$ PAR. These curves were generated on the 3rd leaf for each tree monthly during each growing season. A-I parameters were calculated by fitting the response curves to a non-rectangular hyperbola using non-linear least square regression (Hanson *et al.*, 1987) according to the following equation:

$$Pn = Asat \times \left\{ \left[1 - \left(1 - \frac{R_D}{Asat} \right) \right]^{1 - \frac{PPFD}{LCP}} \right\}$$

where P_n is net photosynthesis at a given light level, A_{sat} is light saturated net photosynthesis, R_D is dark respiration taken during the day, $PPFD$ is photosynthetic photon flux density, and LCP is light compensation point.

From the initial slope of the A-I curve, the maximum apparent quantum efficiency for net CO_2 assimilation (Φ_{CO_2}) was determined using linear regression (Sasek and Richardson, 1989). Assimilation– C_i response curves were also generated at $2000 \mu\text{mol m}^{-2}\text{s}^{-1}$ PAR and CO_2 concentrations ranging from 0 to 1600 ppm. Intercellular CO_2 concentration (C_i) is estimated according to the following equation (von Caemmerer and Farquhar, 1981):

$$C_i = \frac{\left(g_s - \frac{E}{2} \right) C_a - A}{\left(g_s + \frac{E}{2} \right)}$$

where C_i is internal (intercellular) CO_2 concentration, g_s is stomatal conductance, E is transpiration rate, C_a is external CO_2 concentration, and A is measured photosynthesis.

From the initial slope of the A- C_i response curves, carboxylation efficiency (Φ_{CE}) was determined as calculated for Φ_{CO_2} in A-I curve (Sasek and Richardson, 1989). A-I response curves and A- C_i response curves were measured at HRC.

The relationship between P_{nMAX} and visible foliar injury in sensitive black cherry leaves of different ages was determined at the end of the 2000 and 2001 growing

seasons. After three years of collecting data, the correlation between cumulative ozone concentrations and reductions in photosynthetic activities of the sensitive class compared to the tolerant class was determined. This percentage reduction was calculated as

$$\text{Percentage difference (\%)} = \left[\frac{(T - S)}{T} \right] \times 100$$

where T indicates measurements of the tolerant class and S indicates measurements for the sensitive class.

3.2.4. Chlorophyll fluorescence analysis

A PAM-2000 (Heinz Walz, Germany) portable, pulse-modulated fluorometer was used to conduct chlorophyll fluorescence analysis. Fluorescence characteristics were measured on the adaxial surface of the same leaf tissue utilized for gas exchange analysis. Measurements were made monthly during the growing season of each year. In the dark-adapted state, maximum and minimum fluorescence were measured, and then maximum quantum efficiency, F_v/F_m , was calculated. In the light-adapted state, quantum efficiency for PSII, maximum electron transport rate, and photochemical, and nonphotochemical quenching coefficients were calculated as described in detail in section 2.2.4.

3.2.5 Statistical analysis

Three replicate trees of each ozone sensitivity class (sensitive or tolerant) were selected. Two branches from each tree were selected and the 3rd basal leaf of each

branch measured. Statistical analysis of the data was performed with the Statistical Analysis System (SAS Institute, Inc., Cary, NC,). Photosynthetic data as well as chlorophyll fluorescence data were analyzed by analysis of variance with ozone sensitivity as the class variable. Statistical significance was designated at the $P \leq 0.05$ probability level by a single asterisk and the $P \leq 0.01$ level by two asterisks.

3.3 Results

3.3.1 Ozone exposure

Black cherry trees were exposed to seasonal 7-h (09:00-16:00 EST) ambient ozone averages of 51 ppb in 2000 and 2001, and 53 ppb in 2002. The one-hour peak value of ambient ozone was higher in 2002 compared to 2000 and 2001 (**Table 3.1**). The highest one-hour peaks in 2000 and 2001 were recorded in June at 90 ppb and 95 ppb, respectively. The highest one-hour peak in 2002 was recorded in July at 121 ppb (**Figure 3.1**). In 2000 and 2001, ozone concentrations were typically highest in May/June and tended to decrease gradually during the summer. In 2002, highest ozone concentrations occurred in July and tended to remain high throughout August (**Figure 3.1**). This seasonal oxidant pattern resulted in higher SUM00 and SUM40 ozone values in 2002 compared to 2000 and 2001 (**Table 3.1**) The cumulative SUM00 ozone concentration in 2002 was similar to those in 2000 and 2001 through July, but began to diverge by early August (**Figure 3.2**) due to the higher late summer levels in 2002.

Table 3.1 Seasonal means of atmospheric ambient ozone concentrations (ppb) and seasonal cumulative ozone concentrations (ppm h) at HRC for three consecutive years, 2000 to 2002. Values are means \pm s.d.

	2000	2001	2002
7-h means	51 \pm 13	51 \pm 12	53 \pm 13
12-h means	51 \pm 12	51 \pm 11	53 \pm 13
Peak means	58 \pm 13	62 \pm 12	66 \pm 16
Seasonal peak	90	95	121
SUM40 (ppm h)	NA*	67.5	75.8
SUM00 (ppm h)	80.4	81.4	85.0

* NA: not available

Figure 3.1. Daily peaks of atmospheric ambient ozone concentration (ppb) at Horton Research Center (HRC), VA, during the growing season of three consecutive years 2000 through 2002

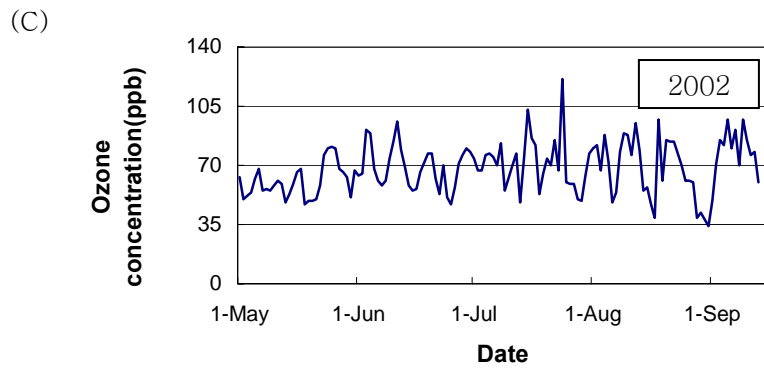
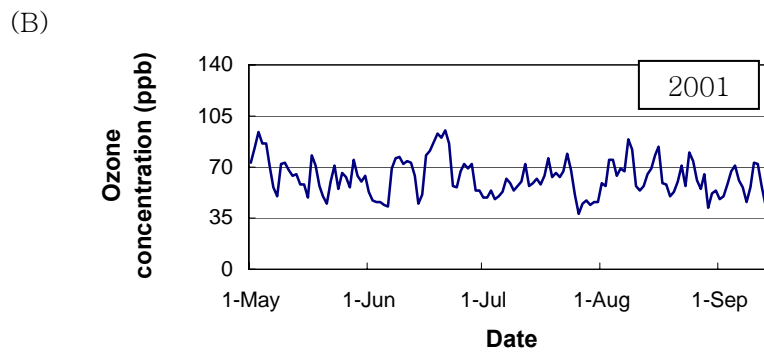
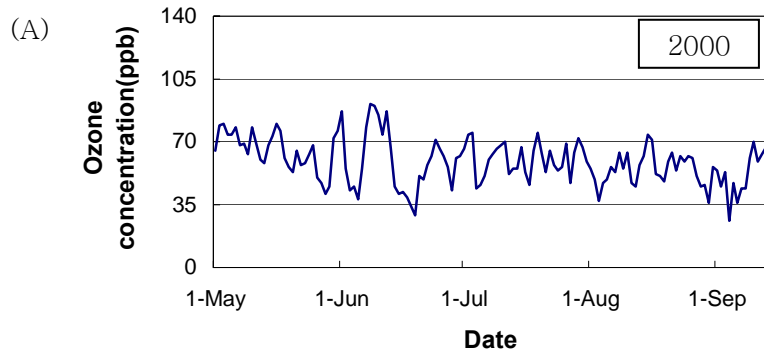
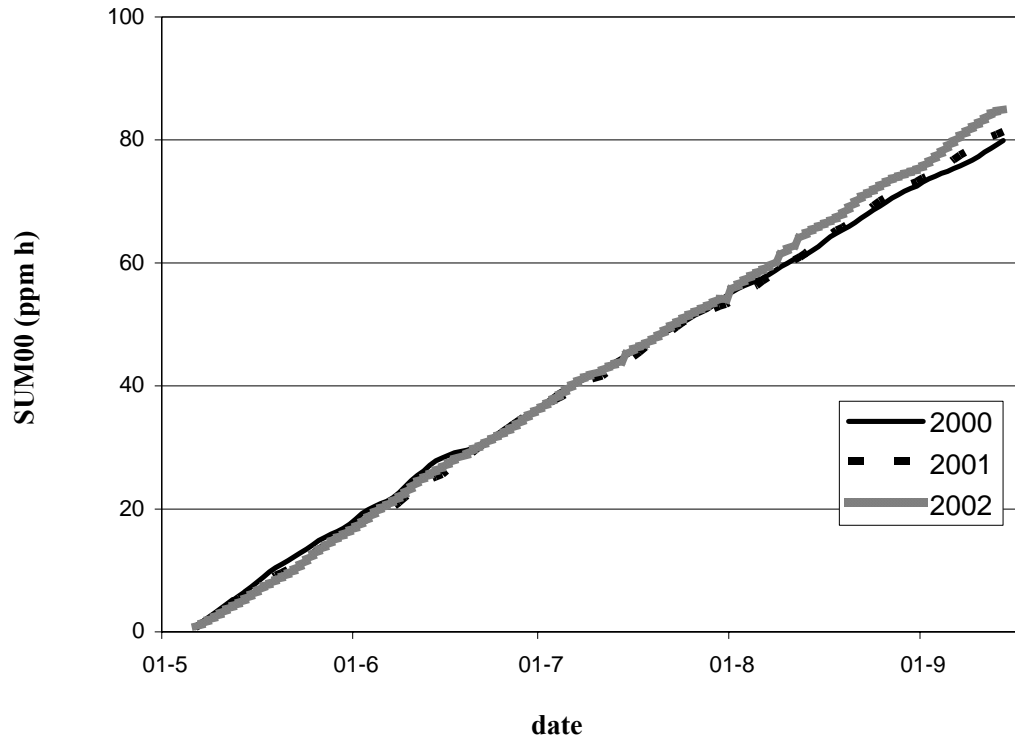


Figure 3.2. Seasonal cumulative ozone concentrations (SUM00, ppm h) for three years 2000 to 2002 at HRC.



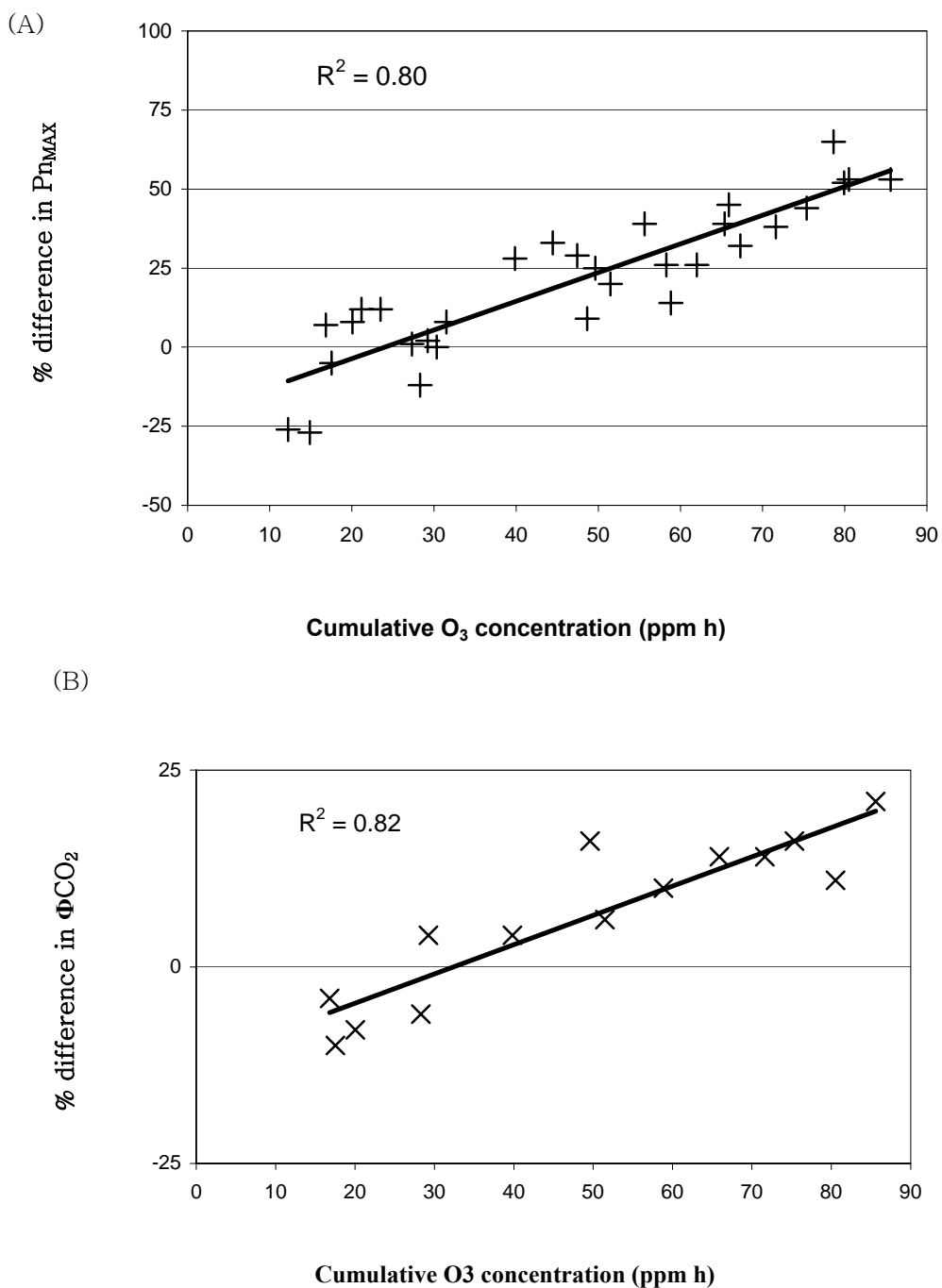
3.3.2. Correlations between cumulative ozone and photosynthetic activities

In all growing seasons, the differences in responses of photosynthetic activities between sensitivity classes in black cherry were evident. The ambient ozone concentrations were sufficiently high to induce reductions of photosynthetic activity in the sensitive class compared to the tolerant class. The reductions of Pn_{MAX} and ΦCO_2 in the sensitive class compared to the tolerant class were highly correlated to seasonal cumulative ambient ozone exposure (SUM00) ($R^2 = 0.80$ for Pn_{MAX} and 0.82 for ΦCO_2) (**Figure 3.3**). Early in the season, Pn_{MAX} and ΦCO_2 of the sensitive class were higher than of the tolerant class. However, later in the growing season, Pn_{MAX} and ΦCO_2 of the sensitive class became lower than of the tolerant class with increased cumulative ozone exposure. The equivalence point between tolerant and sensitive classes for Pn_{MAX} occurred at approximately 22 ppm h (SUM00) (**Figure 3.3A**), whereas equivalence was attained at 32 ppm h for ΦCO_2 (**Figure 3.3B**). This suggests that the dark reactions of photosynthesis are more sensitive to ozone than the light reactions.

3.3.3. Physiological gas exchange

Gas exchange parameters for three years at three different sites are summarized in **Table A.1 (Appendix)**. In May 2000 at the HRC, Pn_{MAX} was significantly higher in sensitive black cherry ($9.16 \mu\text{mol CO}_2 \text{ m}^{-2} \text{ s}^{-1}$) than in tolerant black cherry ($7.42 \mu\text{mol CO}_2 \text{ m}^{-2} \text{ s}^{-1}$). Similarly in May, stomatal conductance (g_s ; $\text{mol H}_2\text{O m}^{-2} \text{ s}^{-1}$) was also significantly higher in sensitive black cherry (0.17 versus $0.10 \text{ mol H}_2\text{O m}^{-2} \text{ s}^{-1}$ in tolerant black cherry). By June, Pn_{MAX} in both sensitive and tolerant black cherry were similar. From June to September, stomatal conductance was not significantly different between sensitive and tolerant black cherry.

Figure 3.3 Percent difference $[100 \times (T-S)/T]$ (A) in Pn_{MAX} (maximum net photosynthetic rates, $\mu\text{mol CO}_2 \text{ m}^{-2} \text{ s}^{-1}$ at $900 \mu\text{mol CO}_2 \text{ m}^{-2} \text{ s}^{-1}$) and (B) in apparent quantum yield for carbon reduction (ΦCO_2 , $\mu\text{mol CO}_2 \mu\text{mol quanta}^{-1}$) in sensitive black cherry compared to tolerant black cherry, as related to cumulative ozone concentration (ppm h). Data collected during the 2000 through 2002 growing seasons at HRC. $n=14$ for ΦCO_2 based on monthly measurements of light response curves. $n=31$ for Pn_{MAX} which includes a second Pn_{MAX} measurement every month.



However, Pn_{MAX} started to decline in sensitive black cherry in July and by September was 60% lower than in tolerant black cherry. Pn_{MAX} in tolerant black cherry remained relatively high at $9.77 \mu\text{mol CO}_2 \text{ m}^{-2} \text{ s}^{-1}$ until August, and then declined slightly as leaves naturally senesced in September. In May, ΦCO_2 was significantly higher in sensitive black cherry than in tolerant black cherry. By September ΦCO_2 was reduced significantly in sensitive black cherry compared to tolerant black cherry. Similar to Pn_{MAX} , ΦCO_2 in tolerant black cherry declined slightly as leaves naturally senesced (**Table 3.2**).

Results were similar at the MTB site. In May 2000, Pn_{MAX} was higher in sensitive ($10.5 \mu\text{mol CO}_2 \text{ m}^{-2} \text{ s}^{-1}$) than in tolerant black cherry ($8.21 \mu\text{mol CO}_2 \text{ m}^{-2} \text{ s}^{-1}$). Stomatal conductance was also higher in sensitive black cherry ($0.15 \text{ mol H}_2\text{O m}^{-2} \text{ s}^{-1}$) compared to tolerant black cherry ($0.13 \text{ mol H}_2\text{O m}^{-2} \text{ s}^{-1}$) in the beginning of the experimental season. Higher Pn_{MAX} and stomatal conductance in sensitive than in tolerant black cherry were maintained until July. In August, Pn_{MAX} and stomatal conductance were 31% and 34%, respectively, lower in sensitive than in tolerant black cherry. In September, 2000, the reductions for sensitive black cherry compared to tolerant black cherry were 50% in Pn_{MAX} and 36% in stomatal conductance (**Table A.1**).

In 2001, only measurements for June and September were taken at only two different sites, HRC and APL. In June at HRC, Pn_{MAX} in both sensitive and tolerant black cherry was very similar at $8.86 \mu\text{mol CO}_2 \text{ m}^{-2} \text{ s}^{-1}$ and $8.36 \mu\text{mol CO}_2 \text{ m}^{-2} \text{ s}^{-1}$ respectively. Likewise, ΦCO_2 was similar for sensitive and tolerant black cherry at 0.053 and $0.049 \mu\text{mol CO}_2 \text{ quanta}^{-1}$. However, in September Pn_{MAX} and ΦCO_2 in sensitive black cherry were significantly reduced (52% and 9%, respectively). In June, stomatal conductance was 11% higher in sensitive ($0.28 \text{ mol H}_2\text{O m}^{-2} \text{ s}^{-1}$) than in tolerant black cherry ($0.24 \text{ mol H}_2\text{O m}^{-2} \text{ s}^{-1}$). In September, stomatal conductance in sensitive black cherry was significantly reduced, while in tolerant black cherry there was little reduction. Stomatal conductance in September was greater in tolerant ($0.22 \text{ mol H}_2\text{O m}^{-2} \text{ s}^{-1}$) than in sensitive black cherry ($0.20 \text{ mol H}_2\text{O m}^{-2} \text{ s}^{-1}$) (**Table 3.3**). Similarly, in June at APL, Pn_{MAX} in both sensitive and tolerant black cherry were similar, $9.28 \mu\text{mol CO}_2 \text{ m}^{-2} \text{ s}^{-1}$ and $8.66 \mu\text{mol CO}_2 \text{ m}^{-2} \text{ s}^{-1}$, respectively. In September, Pn_{MAX} in sensitive black cherry was significantly lower about 36% than in tolerant at which is similar to other sites as well as in the previous year. In June, stomatal

conductance was significantly higher in sensitive black cherry ($0.24 \text{ mol H}_2\text{O m}^{-2} \text{ s}^{-1}$) than in tolerant black cherry ($0.14 \text{ mol H}_2\text{O m}^{-2} \text{ s}^{-1}$). However, in September, stomatal conductance in sensitive black cherry was 22% lower than in tolerant black cherry (**Table A.1**).

For 2002, gas exchange measurements are available from June to August at HRC and only June and July at APL. At HRC, similar to previous data and other sites, $P_{n_{MAX}}$ in both sensitive and tolerant black cherry were not significantly different in June. However, by September $P_{n_{MAX}}$ in sensitive black cherry ($7.35 \text{ } \mu\text{mol CO}_2 \text{ m}^{-2} \text{ s}^{-1}$) was reduced compared to $P_{n_{MAX}}$ in tolerant black cherry ($9.77 \text{ } \mu\text{mol CO}_2 \text{ m}^{-2} \text{ s}^{-1}$). This reduction in $P_{n_{MAX}}$ by seasonal ambient ozone in sensitive compared to tolerant black cherry was as great as 35%. In September, stomatal conductance was more than 50% lower in sensitive ($0.11 \text{ mol H}_2\text{O m}^{-2} \text{ s}^{-1}$) than in tolerant black cherry ($0.22 \text{ mol H}_2\text{O m}^{-2} \text{ s}^{-1}$) by (**Table 3.4**). At APL, $P_{n_{MAX}}$ of both sensitive and tolerant black cherry were not significantly different in June and July. As summarized in **Table 3.5** photosynthetic activities such as $P_{n_{MAX}}$ and stomatal conductance were higher in sensitive than in tolerant black cherry early in the season. However, later in the growing season photosynthetic activities in sensitive black cherry were significantly lower than in tolerant black cherry. These results were similar at all sites.

Analysis of the assimilation-irradiance (A-I) response curves and assimilation- C_i (A- C_i) response curves was focused on the HRC site which is closest to the Air Quality Monitoring facility. The parameters of assimilation-irradiance (A-I) response curves are summarized in **Table 3.6**. In 2000, LCP and R_D were similar for sensitive and tolerant black cherry until August. However, in September LCP and R_D were 50% and 40% respectively, greater in sensitive black cherry than in tolerant black cherry. Likewise, in September 2001, LCP and R_D were 58% and 48% greater in sensitive black cherry than in tolerant black cherry (**Table 3.6**).

A- C_i response curves in 2002 are shown in **Figure 3.4**. P_n , at 200 ppm C_i was reduced in sensitive black cherry compared to tolerant black cherry in July. By August, at even lower C_i conditions, P_n was significantly reduced in sensitive black cherry and reductions in P_n were even greater as C_i concentrations increased. Carboxylation efficiency (Φ_{CE}) in sensitive black cherry was significantly lower in July 2002. By August, this reduction of Φ_{CE} was more than 40% (**Table 3.4**).

Table 3.2 Maximum net photosynthetic rate (Pn_{MAX} , $\mu\text{mol CO}_2 \text{ m}^{-2} \text{ s}^{-1}$ at $900 \mu\text{mol m}^{-2} \text{ s}^{-1}$), stomatal conductance (g_s , $\text{mol H}_2\text{O m}^{-2} \text{ s}^{-1}$), internal CO_2 concentration (C_i , ppm) and apparent quantum yield for CO_2 assimilation (ΦCO_2 , $\mu\text{mol CO}_2 \mu\text{mol quanta}^{-1}$) on the 3rd leaf of black cherry during the growing season of 2000, at HRC. Values are means \pm s.d. Asterisks indicate significant differences between phenotypes. * at $P<0.05$ and ** at $P<0.01$

	<i>May</i>		<i>June</i>		<i>July</i>		<i>August</i>		<i>September</i>	
	<u>Sensitive</u>	<u>Tolerant</u>	<u>Sensitive</u>	<u>Tolerant</u>	<u>Sensitive</u>	<u>Tolerant</u>	<u>Sensitive</u>	<u>Tolerant</u>	<u>Sensitive</u>	<u>Tolerant</u>
Pn_{MAX}	9.16 \pm 0.67	7.42 \pm 0.42**	11.27 \pm 0.94	10.85 \pm 1.5	8.93 \pm 0.25	9.81 \pm 0.42	7.26 \pm 0.93	9.77 \pm 0.93**	2.85 \pm 0.67	8.07 \pm 0.77**
g_s	0.17 \pm 0.02	0.10 \pm 0.01**	0.30 \pm 0.02	0.26 \pm 0.04	0.21 \pm 0.02	0.16 \pm 0.06	0.21 \pm 0.04	0.22 \pm 0.01	0.22 \pm 0.04	0.21 \pm 0.02
C_i	234 \pm 7.2	206 \pm 9.1**	259 \pm 4.2	254 \pm 5.1	256 \pm 6.1	200 \pm 10.8	298 \pm 9.5	278 \pm 5.5*	308 \pm 10.0	273 \pm 4.0**
ΦCO_2	0.050 \pm 0.002	0.046 \pm 0.003	–	–	0.047 \pm 0.001	0.048 \pm 0.002	0.042 \pm 0.002	0.049 \pm 0.002**	0.031	0.039 \pm 0.002**

– data not available

Table 3.3 Maximum net photosynthetic rate (Pn_{MAX} , $\mu\text{mol CO}_2 \text{ m}^{-2} \text{ s}^{-1}$ at $900 \mu\text{mol m}^{-2} \text{ s}^{-1}$), stomatal conductance (g_s , $\text{mol H}_2\text{O m}^{-2} \text{ s}^{-1}$), internal CO_2 concentration (C_i , ppm) and apparent quantum yield for CO_2 assimilation (ΦCO_2 , $\mu\text{mol CO}_2 \mu\text{mol quanta}^{-1}$) on the 3rd leaf of black cherry in June and September, 2001, at HRC. Values are mean \pm s.d. Asterisks indicate significant differences between phenotypes. ** at $P < 0.01$

	<i>June</i>		<i>September</i>	
	<u>Sensitive</u>	<u>Tolerant</u>	<u>Sensitive</u>	<u>Tolerant</u>
Pn_{MAX}	8.86 ± 0.47	8.36 ± 0.22	5.62 ± 0.41	$11.8 \pm 0.75^{**}$
g_s	0.284 ± 0.02	0.246 ± 0.01	0.20 ± 0.01	0.22 ± 0.04
C_i	276 ± 7.2	258 ± 9.1	278 ± 1	$219 \pm 13^{**}$
ΦCO_2	0.053 ± 0.004	0.049 ± 0.002	0.053 ± 0.0005	$0.058 \pm 0.0009^{**}$

Table 3.4 Maximum net photosynthetic rate (Pn_{MAX} , $\mu\text{mol CO}_2 \text{ m}^{-2} \text{ s}^{-1}$ at $900 \mu\text{mol m}^{-2} \text{ s}^{-1}$), stomatal conductance (g_s , $\text{mol H}_2\text{O m}^{-2} \text{ s}^{-1}$), apparent quantum yield for CO_2 assimilation (ΦCO_2 , $\mu\text{mol CO}_2 \mu\text{mol quanta}^{-1}$), and carboxylation efficiency (ΦCE , $\mu\text{mol CO}_2 \text{ ppm CO}_2^{-1}$) on the 3rd leaf of black cherry during growing season of 2002, at HRC. Values are means \pm s.d. Asterisks indicate significant differences between phenotypes. * at $P<0.05$ and ** at $P<0.01$.

	<i>June</i>		<i>July</i>		<i>August</i>	
	<u>Sensitive</u>	<u>Tolerant</u>	<u>Sensitive</u>	<u>Tolerant</u>	<u>Sensitive</u>	<u>Tolerant</u>
Pn_{MAX}	8.48 ± 1.2	9.18 ± 1.13	8.59 ± 1.49	$11.3 \pm 2.11^*$	7.35 ± 0.68	$9.77 \pm 0.93^{**}$
G_s	0.038 ± 0.009	0.04 ± 0.007	0.233 ± 0.03	0.247 ± 0.06	0.106 ± 0.004	$0.22 \pm 0.01^*$
ΦCO_2	0.063 ± 0.005	0.057 ± 0.006	0.052 ± 0.001	$0.061 \pm 0.002^{**}$	0.051 ± 0.003	$0.059 \pm 0.0001^*$
ΦCE			0.026 ± 0.005	$0.035 \pm 0.005^*$	0.023 ± 0.003	$0.039 \pm 0.007^*$

3.3.4. Visible foliar injury

From late July to early August, visible foliar injury became apparent on leaves of sensitive black cherry. By September, most leaves on sensitive black cherry showed visible injury. The symptoms appeared as brown spots on the upper surface of leaves which is typical foliar injury induced by ozone in black cherry (**Figure 3.5**). The estimated foliar injury was more severe in older leaves at 30 to 35% of total leaf area than in younger leaves at 0 to 5% of total leaf area (**Figure 3.6**). The older leaves showed more severe injury in photosynthetic activity than younger leaves in sensitive black cherry. Pn_{MAX} decreased with apparent visible injury as leaves aged in sensitive black cherry measured in September, 2000 and 2001. However, Pn_{MAX} was not significantly different among leaf positions in the absence of any visible injury in tolerant black cherry (**Figure 3.7**). Visible foliar injury was well correlated with photosynthetic activity. Pn_{MAX} was inversely related to percent visible foliar injury with an R^2 value of 0.83 in 2000 and 0.89 in 2001 (**Figure 3.8**). In June of 2002, chlorophyll content was similar between phenotypes. However, in both July and August, chlorophyll content in sensitive black cherry was about 50% lower than in tolerant black cherry (**Figure 3.9A**). In September, visible foliar injury was correlated with chlorophyll content. Chlorophyll content was related inversely to percent visible foliar injury with an R^2 value of 0.95 (**Figure 3.9B**).

3.3.5 Chlorophyll fluorescence

During the experimental season, chlorophyll fluorescence parameters of black cherry were measured monthly and compared between sensitive and tolerant classes for each year 2000 to 2002 (summarized in **Table A.2**, **A.3**, and **A.4** in Appendix). Ambient ozone concentrations caused significant reductions in chlorophyll fluorescence parameters including maximum photochemical efficiency of PSII reaction center (F_v/F_m), quantum yield for PSII (Φ_{PSII}) and photochemical quenching (q_P) in sensitive black cherry by September (**Table A.2**). F_v/F_m was not significantly different between sensitive and tolerant black cherry in June. While this ratio in tolerant trees was maintained around 0.830 throughout the growing season, it declined significantly in September by about 10% in sensitive trees to 0.755 (**Figure 3.10A**). Φ_{PSII} at saturating light intensity was higher in sensitive trees in June.

Table 3.5 Percentage differences of photosynthetic activities (Pn_{MAX} , g_s , C_i , Φ_{CO_2} , and Φ_{CE}) in sensitive black cherry compared to tolerant black cherry. Percentage differences were calculated as $(T-S)/T \times 100$ at three different sites MTR, APL, and HRC, 2000 to 2002.

		<i>May</i>	<i>June</i>	<i>July</i>	<i>August</i>	<i>September</i>
Pn_{MAX}	MTR	-28	-31	-12	31	52
	APL	-	-3	3	-	36
	HRC	-24	-1	17	26	59
g_s	MTR	-16	-26	-21	34	36
	APL	-	-25	-50	-	22
	HRC	-70	-10	-13	28	2
C_i	MTR	-2	2	2	2	-8
	APL	-	-15	-5	-	-8
	HRC	-14	-5	-28	-7	-20
Φ_{CO_2}	HRC	8	-9	9	14	15
Φ_{CE}	HRC	-	11	26	41	-

Table 3.6 Parameters from the assimilation-irradiance (A-I) response curves of tolerant (T) and sensitive (S) black cherry during June to September for three years at HRC. A_{SAT} , assimilation at light saturation ($\mu\text{mol CO}_2 \text{ m}^{-2} \text{ s}^{-1}$ at $1800 \mu\text{mol photon m}^{-2} \text{ s}^{-1}$); LCP, light compensation point ($\mu\text{mol m}^{-2} \text{ s}^{-1}$); R_D , respiration during the day ($\mu\text{mol CO}_2 \text{ m}^{-2} \text{ s}^{-1}$). Values are means \pm s.d.

			<i>June</i>	<i>July</i>	<i>August</i>	<i>September</i>
2000	A_{SAT}	T	8.36 \pm 0.64	9.81 \pm 0.42	10.5 \pm 0.97	8.25 \pm 0.58
		S	8.86 \pm 1.15	10.2 \pm 0.47	6.55 \pm 0.94	3.87 \pm 0.77
	R_D	T	-2.41 \pm 0.03	-1.86 \pm 0.16	-1.66 \pm 0.13	-0.725 \pm 0.15
		S	-2.31 \pm 0.04	-1.78 \pm 0.19	-1.63 \pm 0.08	-1.23 \pm 0.11
	LCP	T	53	33	34	18
		S	49	34	39	36
2001	A_{SAT}	T	10.5 \pm 0.22	NA	NA	12.1 \pm 0.79
		S	9.20 \pm 0.44	NA	NA	5.62 \pm 0.45
	R_D	T	-2.31 \pm 0.11	NA	NA	-1.29 \pm 0.16
		S	-1.47 \pm 0.13	NA	NA	-2.49 \pm 0.12
	LCP	T	53	NA	NA	23
		S	31	NA	NA	55
2002	A_{SAT}	T	10.5 \pm 2.1	12.2 \pm 1.87	12.5 \pm 0.1	NA
		S	9.20 \pm 1.4	8.59 \pm 0.95	7.35 \pm 0.331	NA
	R_D	T	-0.99 \pm 0.14	-1.60 \pm 0.17	-0.892 \pm 0.15	NA
		S	-1.70 \pm 0.06	-1.25 \pm 0.29	-0.563 \pm 0.02	NA
	LCP	T	21	27	18	NA
		S	28	25	13	NA

Figure 3.4 Examples of net assimilation (P_n , $\mu\text{mol CO}_2 \text{ m}^{-2} \text{ s}^{-1}$) - C_i response curves (at $2000 \mu\text{mol m}^{-2} \text{ s}^{-1}$ PAR) on the 3rd leaf of sensitive (closed circles) and tolerant (open circles) black cherry during the growing season of 2002, at HRC. Bars represent \pm one standard deviation and, where not apparent, are contained within symbols.

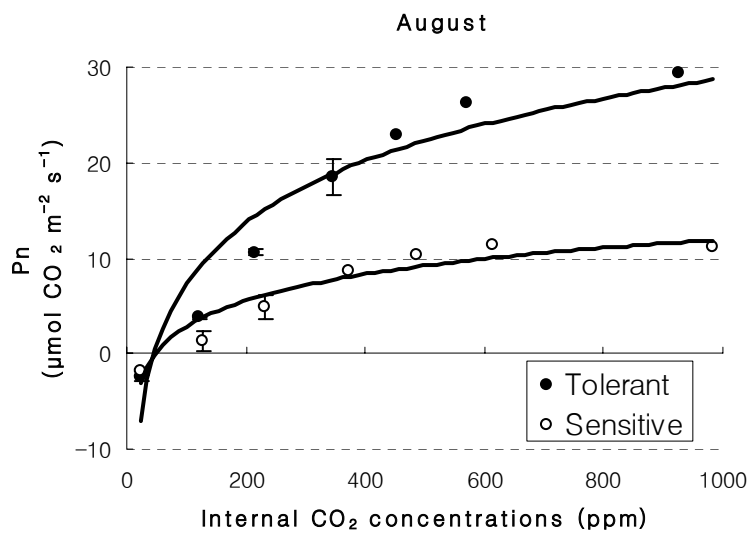
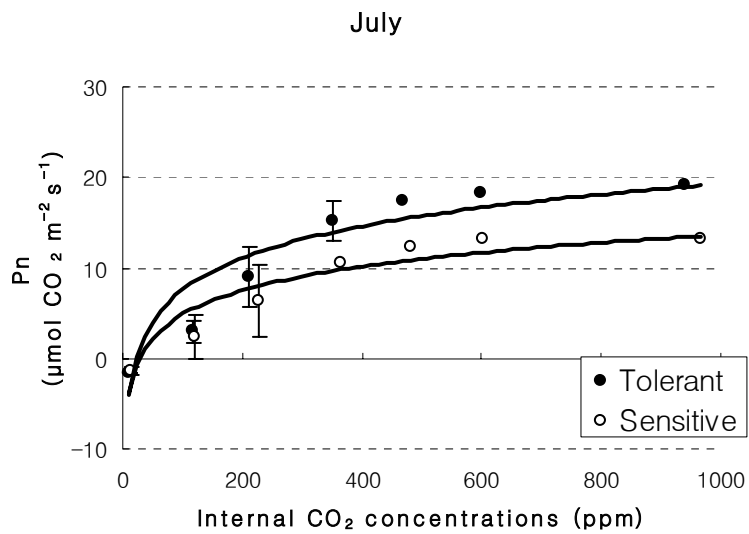


Figure 3.5 Apparent leaf injury developed in sensitive trees in September, 2000 at MTB.



Figure 3.6 Percent visible foliar injury of total leaf area estimated on the different leaf positions of sensitive black cherry in September, 2001, at HRC. Leaf position 10 (L10) is the youngest leaf estimated. Bars represent one standard deviation.

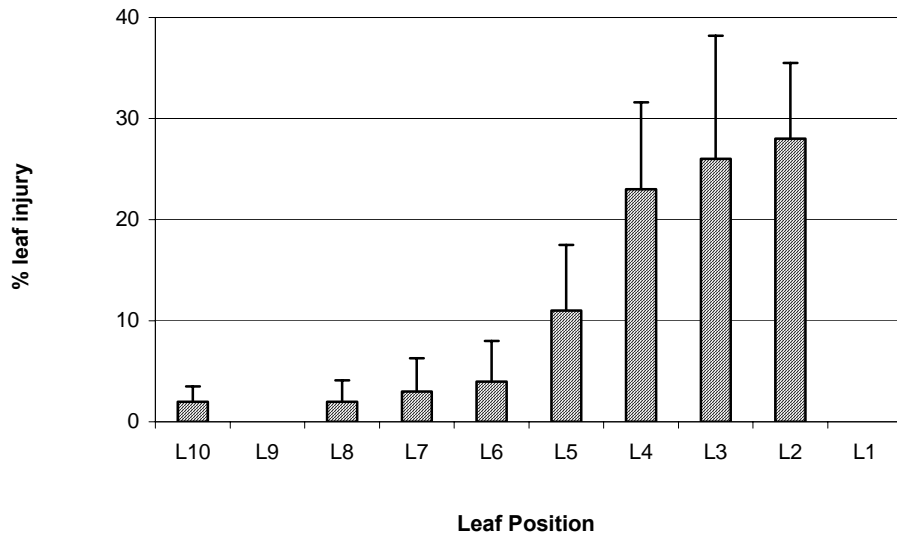
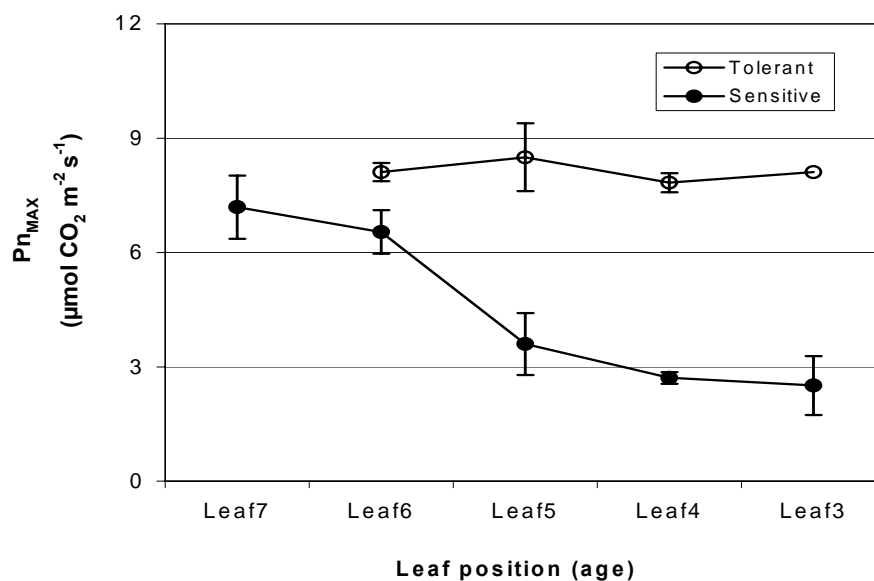


Figure 3.7 Maximum net photosynthetic rate (Pn_{MAX} ; $\mu\text{mol CO}_2 \text{ m}^{-2} \text{ s}^{-1}$ at $900 \mu\text{mol m}^{-2} \text{ s}^{-1}$) on the different leaf positions of sensitive (closed circles) and tolerant (open circles) black cherry in September, (A) 2000 at APL and (B) 2001 at HRC. Leaf position 8 is the youngest leaf measured. Bars represent \pm one standard deviation and, where not apparent, are contained within symbols.

(A)



(B)

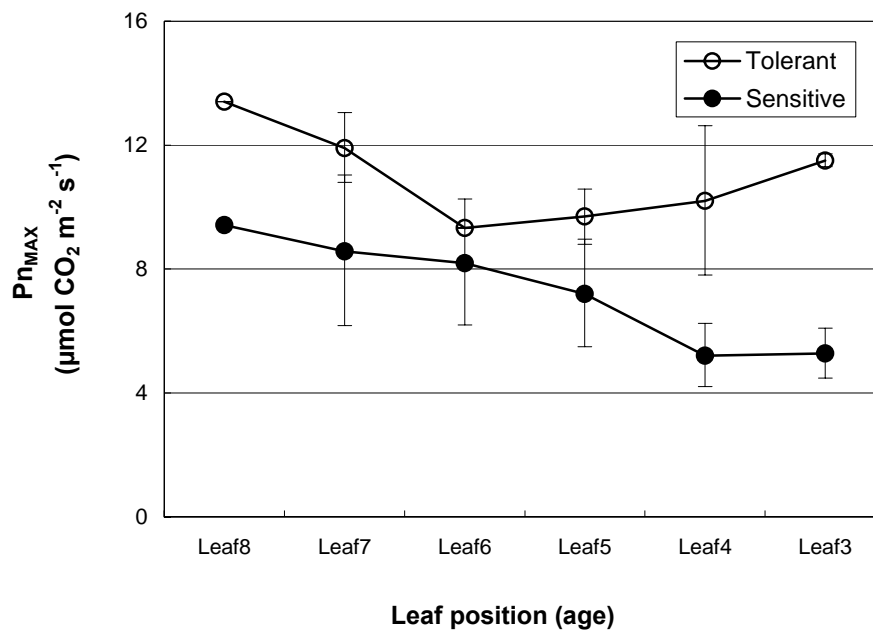


Figure 3.8 Pn_{MAX} (Maximum net photosynthetic rates, $\mu\text{mol CO}_2 \text{ m}^{-2} \text{ s}^{-1}$ at $900 \mu\text{mol m}^{-2} \text{ s}^{-1}$) in relation to percent visible foliar injury of sensitive black cherry in two consecutive years, 2000 (solid line and closed circles) and 2001 (dotted line and open circles), at HRC.

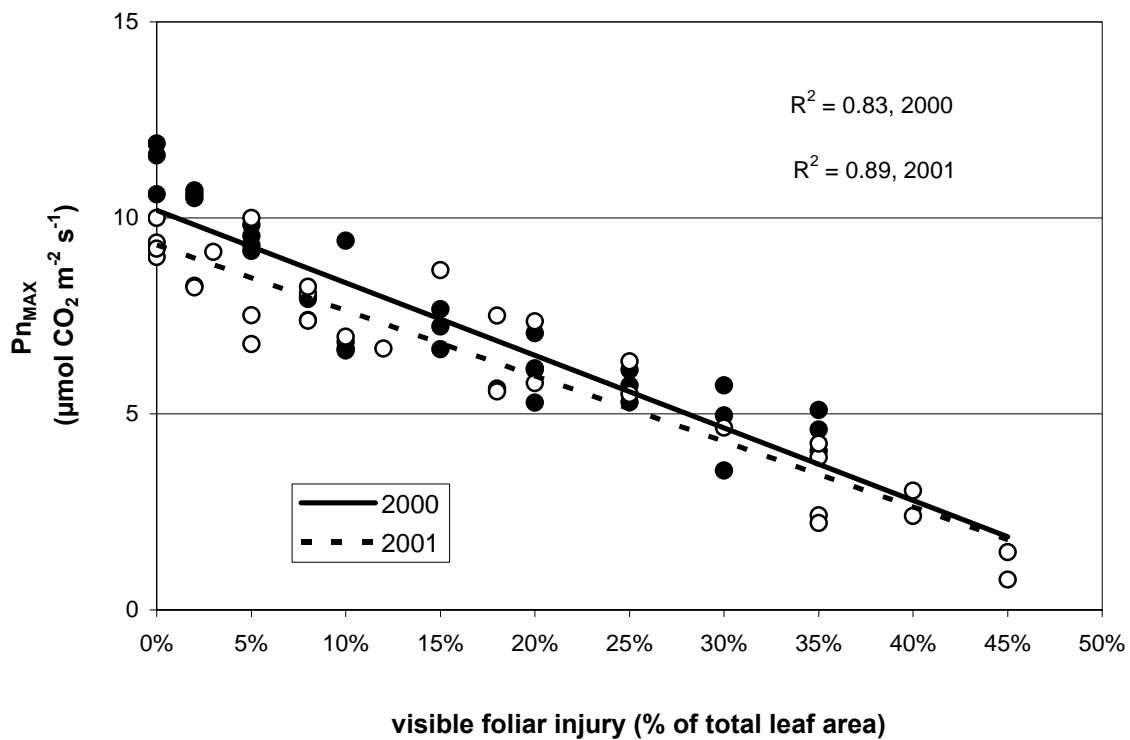
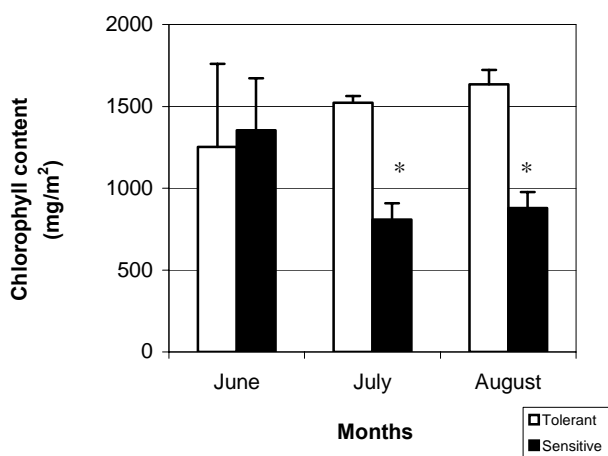
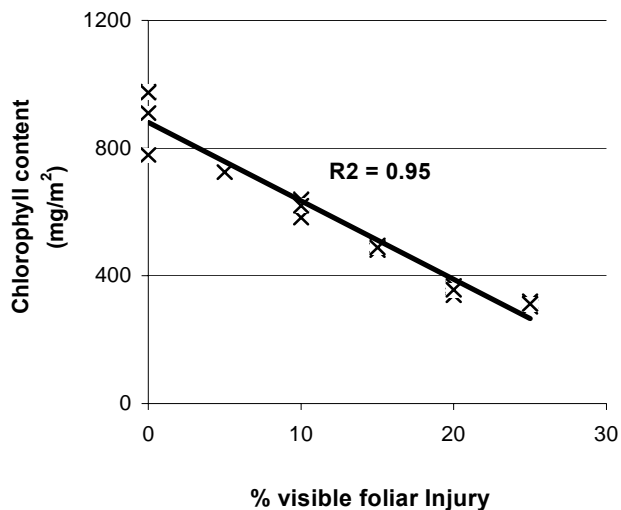


Figure 3.9 (A) Chlorophyll contents on the 3rd leaf of sensitive (black bars) and tolerant (white bars) black cherry during the growing season of 2002, at HRC. (B) Chlorophyll content (mg/m²), in relation to percent visible foliar injury in sensitive black cherry in September, 2002, at HRC. Percent visible injury estimated to the nearest 5%. Each point represents three samples. Bars represent standard deviations. Asterisks indicate significant differences between phenotypes. * at P<0.05 and ** at P<0.01.

(A)



(B)



However, it declined in both tree classes in July. Mild drought or some other environmental stress was suspected as causing this reduction. While Φ_{PSII} started to recover in tolerant black cherry and reached the same level as in June by mid-September, it continued to decline in September in sensitive black cherry. The reduction was more than 50% compared to tolerant black cherry (**Figure 3.10B**). Changes in linear electron transport rate (ETR, $\mu\text{mol electrons m}^{-2}\text{s}^{-1}$) corresponded to changes in Φ_{PSII} . ETR was higher in sensitive black cherry in June. However, it was significantly (50%) lower than in tolerant trees, by September (**Table A.2**).

Similar patterns in chlorophyll fluorescence parameters also occurred in 2001 (**Table A.3**). Ambient ozone concentrations significantly reduced the chlorophyll fluorescence parameters, including Fv/Fm and ETR in sensitive black cherry (**Figure 3.11A** and **Figure 3.11B**). The ratio of Fv/Fm was maintained above 0.8 in tolerant trees throughout the growing season. However, this ratio was significantly reduced in sensitive black cherry as early as July. ETR was also significantly reduced by more than 60% in sensitive black cherry ($45 \mu\text{mol electron m}^{-2}\text{s}^{-1}$) compared to tolerant black cherry ($110 \mu\text{mol electron m}^{-2}\text{s}^{-1}$) in September. The non-photochemical quenching coefficient (qN) increased significantly in July and August in sensitive black cherry (**Figure 3.11C**).

In 2002, the changes in chlorophyll fluorescence parameters for the two sensitivity classes were compared from June to August. In sensitive black cherry, the chlorophyll fluorescence parameters, including maximum photochemical efficiency of PSII reaction centers (Fv/Fm), quantum efficiency for PSII, ETR, and photochemical quenching coefficient of PSII, showed an overall significant reduction, and non-photochemical quenching coefficient of PSII a significant increase in the course of the

season (**Table A.4**). While in tolerant black cherry, Fv/Fm was maintained above 0.80 throughout the growing season, Fv/Fm was significantly reduced, to below 0.80, in sensitive black cherry in July and August (**Figure 3.12A**). The reduction of this ratio indicated the impairment of photochemistry. Percentage changes in sensitive compared to tolerant black cherry in Fv/Fm and its two different components, Fo and Fm are shown in **Figure 3.12B**. In June, Fv/Fm was reduced mostly due to increased Fo; however, in August a lowered Fm was mostly responsible for Fv/Fm reduction. Φ PSII was inhibited as early as June in sensitive trees and did not recover during the growing season (**Figure 3.12C**).

3.4 Discussion

Ambient ozone concentrations and duration of exposures during the experimental seasons of 2000, 2001, and 2002 were great enough to disrupt physiological activity and result in visible foliar injury only in sensitive black cherry. The seasonal 7-h and 12-h ambient ozone concentrations averaged 40 to 50 ppb and episodic peaks reached 90 to 120 ppb. These concentrations typically occur during the summer months in Mid-Atlantic States (Skelly, 2000; Schaub *et al.*, 2003).

Foliar injury was first observed on leaves of sensitive trees in mid-July of each year. The ozone SUM00 dose at this time was about 40 ppm*h. By comparison, seedling black cherry, growing in open plots and monitored daily for initial symptom development, first displayed foliar injury at an AOT40 (Accumulative Ozone Over Threshold 40 ppb) dose of 5 to 6 ppm*h (VanderHeyden *et al.*, 2001). Converting SUM00 to AOT40 yielded an ozone dose of 10.6 ppm*h to produce symptoms in the present study.

Figure 3.10 (A) Maximum photochemical efficiency of PSII ($F_v [F_m - F_o]/F_m$; F_m , maximum fluorescence; F_o , minimum fluorescence) and (B) quantum efficiency for PSII (Φ PSII) on the 3rd leaf of sensitive (closed circles) and tolerant (open circles) black cherry during the growing season, 2000, at HRC. Bars represent \pm one standard deviation. Asterisks indicate significant differences between phenotypes. * at $P < 0.05$ and ** at $P < 0.01$.

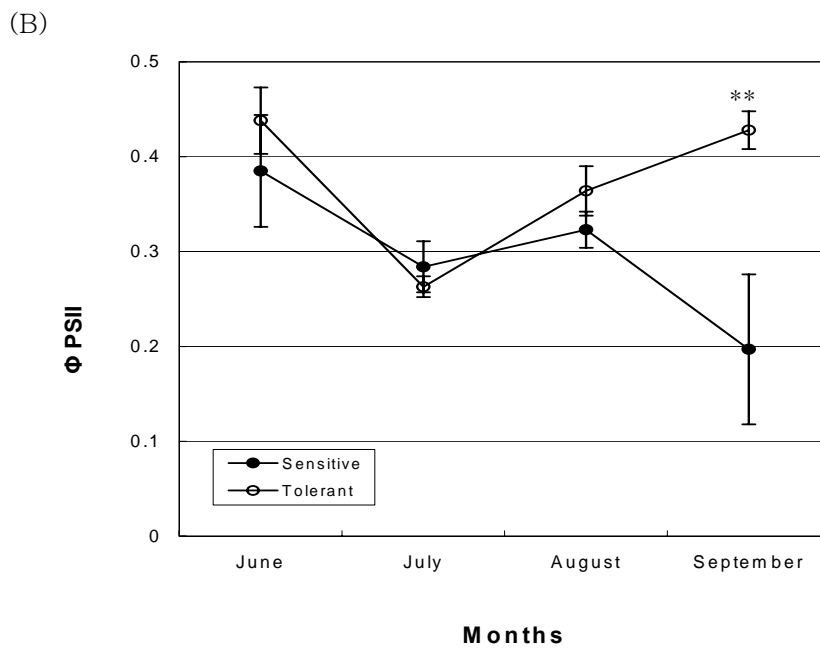
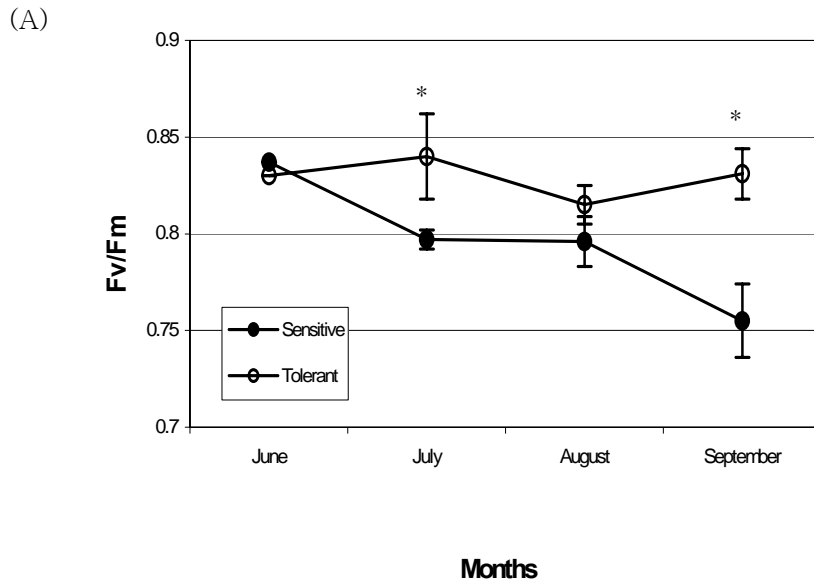
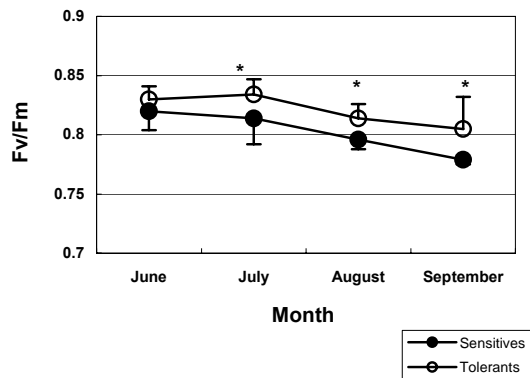
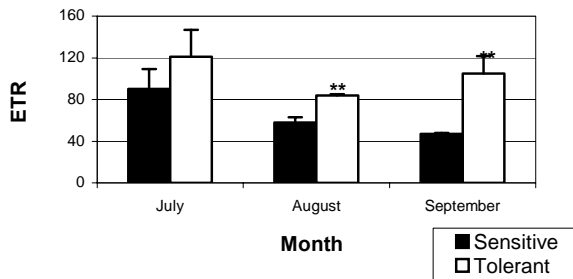


Figure 3.11 (A) Maximum photochemical efficiency of PSII ($F_v[F_m - F_o]/F_m$; F_m , maximum fluorescence; F_o , minimum fluorescence), (B) electron transport rates of PSII (ETR, $\mu\text{mol electrons m}^{-2}\text{s}^{-1}$), and (C) non-photochemical quenching (qN) on the 3rd leaves of sensitive (closed circles and black bars) and tolerant (open circles and white bars) black cherry during the summer of 2001 at HRC. Bars represent \pm one standard deviation. Asterisks indicate significant differences between phenotypes. * at $P < 0.05$ and ** at $P < 0.01$

(A)



(B)



(C)

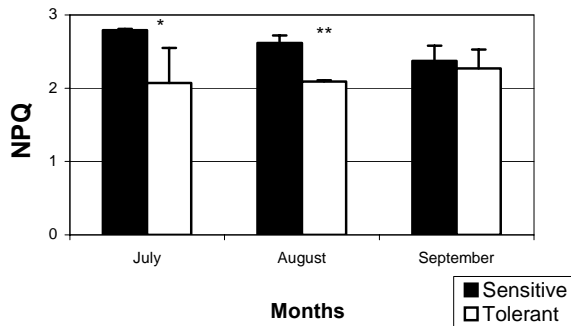
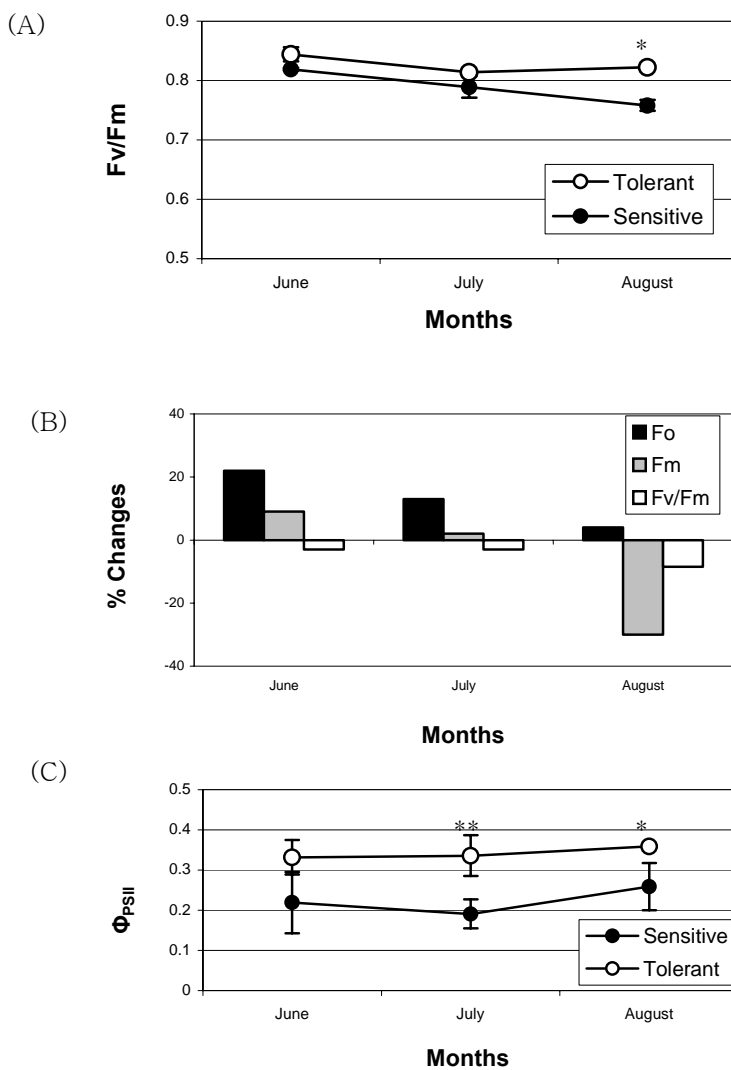


Figure 3.12 (A) Maximum photochemical efficiency of PSII ($F_v [F_m - F_o]/F_m$; F_m , maximum fluorescence; F_o , minimum fluorescence), (B) percentage changes in maximum photochemical efficiency ($F_v [F_m - F_o]/F_m$, white bars) and its components, maximum chlorophyll fluorescence (F_m , grey bars) and minimum chlorophyll fluorescence (F_o , black bars), and (C) quantum efficiency for PSII (Φ_{PSII}) on the 3rd leaf of sensitive (closed circles) and tolerant (open circles) black cherry during the growing season of 2002, at HRC. Bars represent \pm one standard deviation and, where not apparent, are contained within symbols. Asterisks indicate significant differences between phenotypes. * at $P < 0.05$ and ** at $P < 0.01$.



Since observations were made at two-week intervals, rather than daily, symptoms could have appeared a week or more earlier than mid-July. Considering a seasonal 12 hr mean ozone concentration of 51 ppb, symptom appearance one week earlier would result in a AOT40 dose of 6.3 ppm·h indicating trees monitored in the Blacksburg-Giles County area were in the same sensitivity range as those used by VanderHeyden *et al.* (2001). In contrast, Samuelson (1994) did not observe foliar injury on one-year-old black cherry until a SUM00 dose of at least 115 ppm·h was attained, indicating seedlings utilized in that study were highly ozone tolerant.

Reductions in CO₂ assimilation rates, chlorophyll content, and chlorophyll fluorescence parameters, along with the appearance of visible foliar injury, were clearly present in sensitive black cherry, but were not found in tolerant black cherry. Because current ambient concentrations of ozone are high enough to cause damage to plants and concentrations are predicted to increase continuously, it has been suggested that natural selection may occur to enhance tolerance to ozone in forest populations. Studies have identified that genetic variations in sensitivity to ozone exist within several broad-leaved tree species. However, only a few reports have identified evidence of these variances in ozone sensitivity among black cherry genotypes (Kouterick *et al.*, 2000; Lee *et al.*, 2002). The comparison between sensitive and tolerant black cherry in response to ozone has been principally limited to visible foliar injury (Bennett *et al.*, 1992; Skelly, 2000). This present research was focused on identifying the tolerance mechanisms by comparing various physiological responses to ozone between sensitive and tolerant black cherry under field conditions.

The ozone-induced visible foliar injury of sensitive black cherry may be the result of its greater stomatal conductance and consequently greater ozone uptake

compared to tolerant black cherry early in the growing season. Higher ozone uptake with greater stomatal conductance has been linked to greater ozone injury in sensitive black cherry seedlings (Kouterick *et al.*, 2000). This relationship between stomatal conductance and foliar injury was observed early in the growing season in the present study. Tolerant black cherry showed lower stomatal conductance corresponding to lower Pn_{MAX} than sensitive black cherry in May and June. However, from July on, tolerant trees had greater gas exchange rates than sensitive trees (indicating higher ozone uptake) but foliar symptoms were never observed. One possible defense mechanism in tolerant black cherry is to limit ozone uptake. Guidi *et al.* (1998) found that a tolerant clone of poplar showed decreased stomatal conductance in mature leaves when exposed to 150 ppb of ozone for 5 hr. A complete recovery of photosynthetic activity with recovered stomatal conductance occurred when the ozone stress was removed. At present, it has not been evident which process would be affected by ozone first, assimilation or stomatal closure. Many studies have suggested that stomatal closure follows a decline in CO_2 assimilation in order to maintain internal CO_2 concentrations (Reichenauer *et al.*, 1997; Farage and Long, 1999; Bortier *et al.*, 2001). In the present study, it appears that sensitive black cherry has an inherently higher stomatal conductance and photosynthetic rate than tolerant black cherry under low ozone doses, i.e. early in the growing season. However, as the ozone dose increases, sensitive trees are adversely affected whereas tolerant trees are not. Since foliar injury never developed in tolerant leaves, ozone exclusion is not the principal mechanism resulting in tolerance.

Leaf structure has also been implicated in contributing to the differential ozone response between tolerant and sensitive black cherry. Ferdinand *et al.* (2000) compared morphological differences between sensitive and tolerant seedlings and found greater

stomatal density in sensitive compared to tolerant seedlings. This observation suggested a greater potential of higher stomatal conductance in sensitive seedlings.

Evans *et al.* (1996) have reported that certain leaf morphological characteristics such as stomatal density and intercellular air space may lead to increased ozone ingress into leaves and increased internal diffusivity among ozone target cells, such as palisade mesophyll cells. The response to ozone may be underestimated if sensitivity emphasizes only the differences in stomatal conductance (Schaub *et al.*, 2003). Fredericksen *et al.* (1995) reported thinner leaves and a lower palisade/ spongy mesophyll thickness ratio in sensitive black cherry than in tolerant black cherry. According to Ferdinand *et al.* (2000), leaves of R-12, ozone-sensitive seedlings, displayed greater spongy mesophyll with greater intercellular air space and thinner palisade mesophyll than MO-7, ozone-tolerant seedlings. These morphological characteristics in sensitive black cherry would provide less mesophyll resistance to ozone ingress to the palisade mesophyll and may lead to increased dead cells and visible foliar injury.

The relationship between visible foliar injury and photosynthetic function in black cherry has been investigated previously, but no prior studies have been completed with trees growing in a natural environment. Our conclusions are based on a unique combination of observations of foliar injury, chlorophyll fluorescence and gas exchange on the same leaf throughout the growing seasons of three years. In a controlled environment study at 25% of full sunlight, Samuelson (1994) observed a weak trend of decreased photosynthesis with increased leaf injury in one-year-old tolerant seedlings at 2X ambient ozone concentrations and the author concluded “this study confirms the potential for reductions in black cherry ... leaf gas exchange with the identification of visible ozone-induced foliar injury by field studies”. In contrast, no differences in net

photosynthesis were observed between injured and non-injured leaves of seedling and canopy black cherry trees growing in controlled open-top chambers or natural field conditions in other studies (Schaub *et al.*, 2003; Schaub *et al.*, 2005). In the only study utilizing a comparison of tolerant and sensitive black cherry phenotypes, Kouterick *et al.* (2000) reported that the differences in ozone uptake and visible foliar injury between families did not correspond with family differences in photosynthetic activity to ozone exposure. The relatively ozone-sensitive family R-12 had more visible foliar injury on the existing leaves and higher net photosynthesis on the newly expanded leaves than occurred in the relatively ozone-tolerant family MO-7 throughout the growing season of 1994. Net photosynthesis of newly expanded young leaves (third position from the branch tip) was measured throughout the growing season and the cumulative effect of ozone was not considered. Such young leaves would have higher net photosynthesis and would not yet be severely affected by ozone. Our results clearly show, for the first time, that reductions of net photosynthesis in sensitive black cherry compared to tolerant black cherry are correlated with seasonal cumulative ozone concentrations and with the amount of visible foliar injury present on leaf tissue.

Greater foliar injury on the older leaves was observed in sensitive black cherry at the end of the growing season. This was due to a longer duration of ozone exposure than for younger leaves produced later in the growing season. Older leaves also showed more severe injury to maximum photosynthesis than younger leaves in sensitive black cherry. Visible foliar injury was well correlated to photosynthetic activity in this study. The percent leaf injury of total leaf area was negatively related to maximum photosynthesis in sensitive black cherry. Results in this study are supported by many studies of other ozone-sensitive trees and crops that have shown a clear inverse

relationship between visible foliar injury and photosynthetic activity (Davis and Skelly, 1992; Flagler *et al.*, 1994). The existence of the high correlation between visible foliar injury and photosynthetic activity in black cherry sensitivity classes in this study shows that such visible foliar injury could be a simple measure of ozone impacts on different phenotypes in forest ecological studies. These results support the observations of decreased stem biomass and shoot elongation in sensitive black cherry compared to tolerant black cherry in Massachusetts and the southern Lake Michigan area (Vollenweider *et al.*, 2003; Bennett *et al.*, 2006).

Several studies (Chappelka and Samuelson, 1998; Chappelka *et al.*, 1999; Schaub *et al.*, 2003) have demonstrated that local research sites and their environmental factors, including micro-climate, have an important role in determining plant response to ambient ozone levels. Although ambient ozone concentrations, 7-h and 12-h, SUM00 and SUM40, were highest in 2002, the photosynthetic activity of sensitive trees suffered less damage than in other years. On the other hand, in 2000, ambient ozone concentrations were lowest, but damage to photosynthetic activity was greatest. Showman (1991) observed similar results in a field survey of foliar injury occurrence on vegetation and trees in Ohio and Indiana over two years. In 1988, less foliar injury was observed with higher ambient ozone concentrations, whereas in 1989, severe injury was observed with lower ambient ozone concentrations. Showman (cited by Schaub *et al.*, 2003) explained that this result was due to the much lower precipitation in 1988 than 1989.

In the present study, carboxylation efficiency was calculated from the internal CO₂ response curves and compared between sensitive and tolerant trees. Carboxylation efficiency in sensitive specimens was reduced initially in July along with Pn_{MAX}.

However, when CO₂ was not a limiting factor, under saturating conditions, the maximum rate of electron transport used in the regeneration of RUBP was reduced also indicating ozone damage to both light and dark reactions of photosynthesis. A loss of RUBISCO activity and carboxylation capacity has been attributed as the primary cause of a decrease in photosynthetic rate resulting from ozone exposure in other plant species (Reichenauer *et al.*, 1997; Farage and Long, 1999; Shavin *et al.*, 1999; Castagna *et al.*, 2001). In this study, RUBISCO levels were not measured; however, a reduction in carboxylation efficiency was the first response in sensitive black cherry and the primary contributor to lower Pn_{MAX}. The quantum efficiency was highest in sensitive black cherry in June and did not begin to decline until August. Late in the growing season, the reduction in carboxylation efficiency in sensitive trees (40% reduction compared to tolerant) was much higher than the reduction in quantum efficiency (only 14% compared to tolerant). Further research concerning the genetic variation of ozone sensitivity among black cherry should include examinations of biochemical components such as anti-oxidant production and RUBISCO activity levels which may differ in ozone sensitivity relative to foliar injury.

Chlorophyll fluorescence data suggest that the light reactions are also altered in sensitive black cherry. The depression in Fv/Fm indicates that the efficiency in energy conversion of PSII was damaged. Two different parameters are responsible for light reaction impairments. Initially, mainly increased Fo caused decreased Fv/Fm in sensitive black cherry which suggests that the transport of excitation energy from light-harvesting complexes to reaction centers was impaired. However, late in the growing season, the main cause of Fv/Fm was decreased Fm, which suggests that linear electron transport from the reaction center of PSII to PSI was impaired. Along with the reduction

in chlorophyll fluorescence, decreased CO₂ assimilation was observed in sensitive trees as early as in July. However, there was a larger decrease in CO₂ assimilation rate (more than 25% decrease compared to tolerant) than chlorophyll fluorescence (less than 10 % decrease) in sensitive trees. This indicates that there are electron sinks other than carbon assimilation (Soja *et al.*, 1998; Bortier *et al.*, 2001). Increased qN with correspondent decreased qP in sensitive compared to tolerant black cherry observed in June and July indicates a non-radiative dissipation of energy as heat (Krause and Weis, 1991; Bolhar-Nordenkamp *et al.*, 1989; Lorenzini *et al.*, 1999). Mechanisms of qN are still uncertain; however, many of its characteristics are generally accepted. One of the generally accepted characteristics is the so called xanthophylls cycle, where violaxanthin is converted to zeaxanthin via the intermediate of antheraxanthin. This reaction is accelerated by increasing the trans-thylakoid pH gradient generated by high light and activating the violaxanthin de-epoxidase enzyme (Dall'Osto *et al.*, 2005).

The reductions in assimilation rates occurred with loss in chlorophyll concentration of the leaves in sensitive black cherry in July. Under ambient ozone concentrations, accelerated senescence as well as accelerated autumn coloring in sensitive species was frequently observed late in the growing season (Skarby *et al.*, 1998; Günthardt-Goerg *et al.*, 1999). It is also evident when fumigation occurs with high concentration of ozone (Tenga *et al.*, 1993; Yun and Laurence, 1999). However, how much reduction in assimilate is caused by loss of chlorophyll content is still uncertain. It is assumed that a loss of chlorophyll content may lead to a reduction in light harvesting. It is true that a loss of chlorophyll can lead to a decrease in net assimilation if light is limited and chlorophyll is not sufficient to capture the limited light energy. Also, if chlorophyll loss is coupled with a reduced efficiency of

photosynthetic energy conversion, it may lead to decreased net assimilation (Bortier *et al.*, 2001). However, the opposite effect was reported by Adams *et al.* (1990); although chlorophyll content was reduced, the continued efficient use of the light captured by the remaining chlorophyll was observed. In this present study, a negative relationship between chlorophyll content and percent leaf injury and the correspondent decreased assimilation rate in sensitive black cherry was clearly evident.

Maximum net photosynthesis and quantum yield for CO₂ assimilation (Φ_{CO_2}) decreased dramatically with apparent visible ozone symptoms in sensitive trees at the end of the growing season each year. Tolerant trees showed minimal decreases in maximum photosynthesis and Φ_{CO_2} as the leaf aged in the absence of any visible symptoms. Maximum electron transport rate (ETR) and quantum yield of PSII (Φ_{PSII}) also decreased in symptomatic sensitive trees at the end of growing season each year. Maximum photochemical efficiency (Fv/Fm) in sensitive trees was severely damaged by ambient ozone concentrations. This decline was due to both increased Fo and decreased Fm. In the light reaction apparatus, the production of electrons by the water splitting reaction in PSII (electron generation site of PSII) was first impaired in June and then electron transport PSII to PSI (electron donor site of PSII) was damaged by August.

This study is the first demonstration of a linear relationship between a decrease in photosynthesis and an increase in ozone-induced foliar injury in black cherry and the characterization of the different physiological responses of the carbon assimilation system of tolerant and sensitive phenotypes under field conditions with current ambient ozone concentrations. The dark reactions of photosynthesis were found to be more sensitive to ozone than in the light reactions. The production of electrons by the water

splitting reaction of PSII was the initial site of ozone damage in the light reaction apparatus.

Chapter 4

4.1 Conclusion

Two different ozone exposure regimes and two very different species, an annual crop and a perennial tree species were utilized in this study: an acute short-term ozone exposure on tobacco and a chronic exposure of current ambient ozone levels on black cherry. Observations are summarized in **Table 4.1**. In both studies, phenotypes with contrasting sensitivities were used. Prior to ozone exposure, the sensitive phenotypes of black cherry showed higher photosynthetic activity with higher stomatal conductance and a higher electron transport rate than the tolerant trees. This suggests that sensitive black cherry had a greater potential for ozone uptake and the capacity to generate more severe oxidative stress than tolerant black cherry. However, in tobacco, the tolerant cultivar had higher photosynthetic activities with higher stomatal conductance and a lower electron transport rate than the sensitive cultivar, suggesting the tolerant cultivar had a greater potential for ozone uptake and the capacity to generate more severe oxidative stress. With exposure to high ozone concentration, the tolerant tobacco cultivar showed less immediate reduction in net photosynthetic activity and a rapid recovery compared to the sensitive cultivar, suggesting the existence of efficient scavenging systems of oxidative stress.

Acute short-term exposure to 200 ppb ozone for 4 hr caused severe decreases of physiological function in Bel-B, the tolerant tobacco cultivar. However, recovery of those physiological functions was evident at 24 hr post-fumigation. On the other hand, Bel-W3, the extremely sensitive cultivar, showed irreversible impairment in PSII reaction centers and eventual cell death. Acute exposure to high ozone concentration caused greater damage to the light reaction apparatus than the dark reaction of CO₂

assimilation in ozone-sensitive tobacco. The immediate and substantial impairment of physiological performance by ozone and the subsequent rapid recovery supports a cellular tolerance mechanism directed towards repair/synthesis of damaged cellular components in the ozone-tolerant cultivar.

Ozone-sensitive black cherry developed visible symptoms as well as impairment in physiological functions in response to cumulative atmospheric ozone exposure. However, ozone-tolerant black cherry showed minimal decreases in physiological functions with the absence of any visible symptoms as leaves aged. In black cherry, the dark reactions were more sensitive to ozone than the light reactions, suggesting that electron sinks other than CO₂ assimilation can function to prevent over-reduction of the photosystem.

In the light reaction apparatus in sensitive black cherry, the production of excitation by the water splitting reaction in PSII was first impaired, then electron transport from PSII to PSI, represented by increasing F_0 in June, then decreasing F_m in August. The impairment of the production of excitation by the water splitting reaction in PSII was also observed in ozone-tolerant tobacco in the response to acute ozone exposure. Ozone-sensitive tobacco showed a direct impairment of electron transport from PSII to PSI with considerable loss of pigments.

In tobacco, the photosystem appeared to be more sensitive to ozone than the dark reactions, whereas the opposite was true for black cherry. This may be due to an acute versus a chronic ozone exposure. Fumigating black cherry seedlings with an acute concentration or tobacco with a chronic concentration could validate this suggestion.

Table 4.1 Comparison of response of tobacco to acute ozone exposure with that of black cherry to chronic ozone exposure

	Tobacco (<i>Nicotiana tabacum</i>)	Black cherry (<i>Prunus serotina</i>)
Ozone exposure	Acute exposure to high ozone concentration	Chronic exposure to current ambient ozone concentration
Plant species	Annual crop species	Perennial tree species
Prior to ozone exposure	Tolerant cultivar Higher photosynthetic activity with higher stomatal conductance - Greater potential for more ozone uptake and the capacity to generate more severe oxidative stress	Sensitive tree Higher photosynthetic activity with higher stomatal conductance - Greater potential for more ozone uptake and the capacity to generate more severe oxidative stress
Measurements taken and compared	4 th leaf position from apical tip	3 rd basal leaf position
Visible symptoms	Less than 5% in tolerant cultivar 35% in sensitive cultivar	No visible symptom in tolerant tree 30% in sensitive tree
Photosynthetic Activities	<ul style="list-style-type: none"> - Immediate reduction in both cultivars - Greater reduction rate in sensitive cultivar than tolerant cultivar - Rapid recovery in 24 hr occurred only in tolerant cultivar - No recovery in sensitive cultivar - Greater reduction in light reaction than C assimilation : light reaction was more susceptible 	<ul style="list-style-type: none"> - Greater photosynthetic activity in sensitive tree early season - With increasing cumulative ozone, photosynthetic activity in sensitive tree reduced compared to tolerant tree - Tolerant tree maintained photosynthetic activity throughout growing season - Pn_{MAX} decreased earlier than ΦCO₂ : C assimilation was more susceptible than light reaction
Parameters impact to Fv/Fm	<ul style="list-style-type: none"> - Increased Fo in tolerant cultivar - Decreased Fm in sensitive cultivar - Water splitting site was altered first then electron transport from PSII to PSI 	<ul style="list-style-type: none"> - Increased Fo in sensitive phenotype in early growing season - Decreased Fm in sensitive late growing season - Water splitting site was altered first then electron transport from PSII to PSI

References

- Adams MB, Edwards NT, Taylor GE** (1990) Whole plant ¹⁴C-photosynthate allocation in *Pinus taeda*: seasonal patterns at ambient and elevated ozone levels. *Canadian Journal of Forest Research* **20**: 152-158
- Allen RD** (1995) Dissection of oxidative stress tolerance using transgenic plants. *Plant Physiology* **107**: 1049-1054
- Antonielli M, Pasqualini S, Ederli L, Batini MS, Loreto F** (1997) Physiological characteristics of tobacco cultivars with contrasting sensitivity to ozone. *Environmental and Experimental Botany* **38**: 271-277
- Barnes JD, Balaguer L, Manrique R, Elvira S, Davison AW** (1992) A reappraisal of the use of DMSO for the extraction and determination of chlorophyll a and b in lichens and higher plants. *Environmental and Experimental Botany* **32**: 85-100
- Bennett JP, Jepsen EA, Roth JA** (2006) Field responses of *Prunus serotina* and *Asclepias syriaca* to ozone around southern Lake Michigan. *Environmental Pollution* **142**: 354-366
- Bennett JP, Rassat P, Berrang P, Karnosky D** (1992) Relationship between leaf anatomy and ozone sensitivity of *Fraxinus pennsylvanica* March. and *Prunus serotina* Ehrh. *Environmental and Experimental Botany* **32**: 33-41
- Bobbink R, Hornung M, Roelofs JGM** (1998) The effects of air-borne nitrogen pollutants on species diversity in natural and semi-natural European vegetation. *Journal of Ecology* **86**: 717-728
- Bolhar-Nordenkampf HR, Long SP, Baker NR, Oquist G, Schreiber U, Lechner EG** (1989) Chlorophyll fluorescence as a probe of the photosynthetic competence of leaves in the field: a review of current instrumentation. *Functional Ecology* **3**: 477-514

- Bortier K, Vandermeiren K, De Temmerman L, Ceulemans R** (2001) Growth, photosynthesis and ozone uptake of young beech (*Fagus sylvatica* L.) in response to different ozone exposures. *Trees* **15**: 75-82
- Bussotti F, Schaub M, Cozzi A, Krauchi N, Feretti M, Novak K, Skelly JM** (2003) Assessment of ozone visible symptoms in the field: Perspectives of quality control. *Environmental Pollution* **125**: 81-89
- Castagna A, Nali C, Ciompi S, Lorenzini G, Soldatini GF, Ranieri A** (2001) Ozone exposure affects photosynthesis of pumpkin (*Cucurbita pepo*) plants. *New Phytologist* **152**: 223-229
- Chameides ML, Kasibhatla PS, Yienger J, Levy HL** (1994) Growth of continental-scale metro-agro-plexes, regional ozone pollution, and world food production. *Science* **264**: 74-77
- Chappelka A, Skelly J, Somers G, Renfro J, Hilderbrand E** (1999) Mature black cherry used as a bioindicator of ozone injury. *Water, Air, and Soil Pollution* **116**: 261-266
- Chappelka AH, Renfro J, Somers G, Nash B** (1997) Evaluation of ozone injury of foliage of black cherry (*Prunus serotina*) and tall milkweed (*Asclepias exaltata*) in Great Smoky Mountains National Park. *Environmental Pollution* **95**: 13-18
- Chappelka AH and Samuelson LJ** (1998) Ambient ozone effects on forest trees of the eastern United States: A review. *New Phytologist* **139**: 91-108
- Clark AJ, Landolt W, Bucher JB, Strasser RJ** (2000) Beech (*Fagus sylvatica*) response to ozone exposure assessed with a chlorophyll a fluorescence performance index. *Environmental Pollution* **109**: 501-507
- Coulston JW, Smith GC, Smith WD** (2003) Regional assessment of ozone sensitive tree species using bioindicator plants. *Environmental Monitoring and Assessment* **83**: 113-127

- Daley PF** (1995) Chlorophyll fluorescence analysis and imaging in plant stress and disease. *Canadian Journal of Plant Pathology* **17**: 167-173
- Dall'Osto L, Caffarri S, Bassi R** (2005) A mechanism of nonphotochemical energy dissipation, independent from PsbS, revealed by a conformational change in the antenna protein CP26. *Plant Cell* **17**: 1217-1232
- Darrall NM** (1989) The effect of air pollutants on physiological processes in plants. *Plant, Cell and Environment* **12**: 1-30
- Davis DD, Miller CA, Coppolino JB** (1977) Foliar response of eleven woody species to ozone with emphasis on black cherry. *Phytopathology* **67**: 185-189
- Davis DD and Skelly JM** (1992) Growth response of four species of eastern hardwood tree seedlings exposed to ozone, acidic precipitation, and sulfur dioxide. *Journal of the Air and Waste Management Association* **42**: 309-311
- Davison AW and Barnes JD** (1998) Effects of ozone on wild plants. *New Phytologist* **139**: 135-151
- Degl'Innocenti E, Guidi L, Soldatini GF** (2002) Characterization of the photosynthetic response of tobacco leaves to ozone: CO₂ assimilation and chlorophyll fluorescence. *Journal of Plant Physiology* **159**: 845-853
- D'Haese D, Vandermeiren K, Asard H, Horemans N** (2005) Other factors than apoplastic ascorbate contribute to the differential ozone tolerance of two clones of *Trifolium repens* L. *Plant, Cell and Environment* **28**: 623-632
- Evans LS, Albury K, Jennings N** (1996) Relationships between anatomical characteristics and ozone sensitivity of leaves of several herbaceous dicotyledonous plant species at Great Smoky Mountains National Park. *Environmental and Experimental Botany* **36**: 413-420
- Farage PK and Long SP** (1999) The effects of O₃ fumigation during leaf development on photosynthesis of wheat and pea: an in vivo analysis. *Photosynthesis Research* **59**: 1-7

- Ferdinand JA, Fredericksen TS, Kouterick KB, Skelly JM** (2000) Leaf morphology and ozone sensitivity of two open pollinated genotypes of black cherry (*Prunus serotina*) seedlings. *Environmental Pollution* **108**: 297-302
- Flagler RB, Lock JE, Elsik CG** (1994) Leaf-level and whole-plant gas exchange characteristics of shortleaf pine exposed to ozone and simulated acid rain. *Tree Physiology* **14**: 361-374
- Foyer CH, Descourvieres P, Kunert KJ** (1994) Protection against oxygen radicals: an important defense mechanism studied in transgenic plants. *Plant, Cell and Environment* **17**: 507-523
- Fredericksen TS, Joyce BJ, Skelly JM, Steiner KC, Kolb TE, Kouterick KB, Savage JE, Snyder KR** (1995) Physiology, morphology, and ozone uptake of leaves of black cherry seedlings, saplings, and canopy trees. *Environmental Pollution* **89**: 273-283
- Fredericksen TS, Skelly JM, Steiner KC, Kolb TE, Kouterick KB** (1996) Size-mediated foliar response to ozone in black cherry trees. *Environmental Pollution* **91**: 53-63
- Genty B, Wonders J, Baker NR** (1990) Non-photochemical quenching of F_0 in leaves is emission wavelength dependent; consequences for quenching analysis and its interpretation. *Photosynthesis Research* **26**: 133-139
- Guidi L, Nali C, Lorenzini G, Soldatini GF** (1998) Photosynthetic response to ozone of two poplar clones showing different sensitivity. *Chemosphere* **36**: 657-662
- Guidi L, Nali C, Ciompi S, Lorenzini G, and Soldatini GF** (1997) The use of chlorophyll fluorescence and leaf gas exchange as methods for studying the different responses to ozone of two bean cultivars. *Journal of Experimental Botany* **48**:173-179
- Günthardt-Goerg MS, Maurer S, Bolliger J, Clark AJ, Landolt W, Bucher JB** (1999) Responses of young trees (five species in a chamber exposure) to near ambient ozone concentrations. *Water, Air, and Soil Pollution* **116**: 323-332

- Gupta SA, Alscher RG, McCune D** (1991) Response of photosynthesis and cellular antioxidants to ozone in *Populus* leaves. *Plant Physiology* **96**: 650-655
- Habash DZ, Parry MAJ, Parmer S, Paul MJ, Driscoll S, Knight J, Gray JC, Lawlor DW** (1996) The regulation of component processes of photosynthesis in transgenic tobacco with decreased phosphoribulokinase activity. *Photosynthesis Research* **49**: 159-167
- Hanson PJ, McRoberts RE, Isebrands JG, Dixon RK** (1987) An optimal sampling strategy for determining CO₂ exchange rate as a function of photosynthetic photon flux density. *Photosynthetica* **21**: 98-101
- Heath RL** (1994) Possible mechanisms for the inhibition of photosynthesis by ozone. *Photosynthesis Research* **39**: 439-451
- Heath RL** (1999) Biochemical processes in an ecosystem: How should they be measured? *Water, Air, and Soil Pollution* **116**: 279-298
- Heggstad HE** (1991) Origin of Bel-W3, Bel-C, and Bel-B tobacco varieties and their use as indicators of ozone. *Environmental Pollution* **74**: 264-291
- Hilderbrand ES, Skelly JM, Fredericksen T** (1996) Incidence of ozone-induced foliar injury on sensitive hardwood tree species from 1991-1993 in Shenandoah National Park, Virginia. *Canadian Journal of Forest Research* **26**: 658-669
- Horton P and Ruban AV** (1993) DELTA pH dependent quenching of the Fo level of chlorophyll fluorescence in spinach. *Biochimica et Biophysica Acta* **1142**: 203-206
- Kangasjärvi J, Talvinen J, Utriainen M, Karjalainen R** (1994) Plant defense systems induced by ozone. *Plant, Cell and Environment* **17**: 783-794
- Kerstiens G and Lenzian KJ** (1989) Interactions between ozone and plant cuticles: II. Water permeability. *New Phytologist* **112**: 21-27

- Kolb TE, Fredericksen TS, Steiner KC, Skelly JM** (1997) Issues in scaling tree size and age responses to ozone; a review. *Environmental Pollution* **98**: 195-208
- Kouterick KB, Skelly JM, Fredericksen TS, Steiner KC, Kolb TE, Ferdinand JA** (2000) Foliar injury, leaf gas exchange and biomass responses of black cherry (*Prunus serotina* Ehrh.) half-sibling families to ozone exposure. *Environmental Pollution* **107**: 117-126
- Krause GH and Weis E** (1991) Chlorophyll fluorescence and photosynthesis: the basics. *Annual Review of Plant Physiology and Plant Molecular Biology* **42**: 313-349
- Krupa SV, Manning WJ, Nosal M** (1993) Use of tobacco cultivars as bioindicators of ambient ozone pollution: an analysis of exposure-response relationships. *Environmental Pollution* **81**: 137-146
- Laisk A and Walker DA** (1989) A mathematical model of electron transport. Thermodynamic necessity for photosystem II regulation; 'light stomata'. *Proceedings of the Royal Society of London Series B* **237**: 417-444
- Langebartels C, Ernst D, Heller W, Lutz C, Payer HD, Sandermann HJ** (1997) Ozone responses of trees: results from controlled chamber exposures at the GSF phytotron. *In: Forest decline and ozone: A Comparison of Controlled Chamber and Field Experiments*. Springer, Berlin, New York, pp 163-200
- Langebartels, C., Wohlgemuth, H., Kschieschan, S., Grün, S., Sandermann, H.** (2002) Oxidative burst and cell death in ozone-exposed plants. *Plant Physiology and Biochemistry*. **40**: 567-575
- Lee EH, Tingey DT, Hogsett WE** (1988) Evaluation of ozone exposure indices in exposure-response modeling. *Environmental Pollution* **53**: 43-62
- Lee JC, Steiner KC, Zhang JW, Skelly JM** (2002) Heritability of ozone sensitivity in open-pollinated families of black cherry (*Prunus serotina* Ehrh.). *Forest Science* **48**: 111-117

- Lesser VM, Rawlings JO, Spruill SE, Somerville MC** (1990) Ozone effects on agricultural crops: statistical methodologies and estimated dose-response relationships. *Crop Science* **30**: 148-155
- Loats KV and Rebbeck J** (1999) Interactive effects of ozone and elevated carbon dioxide on the growth and physiology of black cherry, green ash, and yellow-poplar seedling. *Environmental Pollution* **106**: 237-248
- Lorenzini G, Nali C, Ligasacchi G, Ambrogi R** (1999) Effects of ozone on photosynthesis of Mediterranean urban ornamental plants. *Acta Horticulturae* **496**: 335-338
- Loreto F, Di Marco G, Tricoli D, Sharkey TD** (1994) Measurements of mesophyll conductance, photosynthetic electron transport and alternative electron sinks of field grown wheat leaves. *Photosynthesis Research* **41**: 397-403
- Menser HA, Heggstad HE, Grosso JJ** (1966) Carbon filter prevents ozone fleck and premature senescence of tobacco leaves. *Phytopathology* **56**: 466-467
- Neufeld HS, Lee EH, Renfro JR, Hacker WD, Yu B-H** (1995) Sensitivity of seedlings of black cherry (*Prunus serotina* Ehrh.) to ozone in Great Smoky Mountains National Park I. Exposure-response curves for biomass. *New Phytologist* **130**: 447-459
- Nilsen ET and Orcutt DM** (1996) Atmospheric pollution: SO₂, O₃, NO₂ and “green house gases” *In: Physiology of Plants Under Stress- Abiotic Factors*. John Wiley and Sons New York, NY, pp 518-552
- Orendovici T, Skelly JM, Ferdinand JA, Savage JE, Sanz M-J, Smith GC** (2003) Response of native plants of northeastern United States and southern Spain to ozone exposures; determining exposure/response relationships. *Environmental Pollution* **125**: 31-40
- Pell EJ, Eckardt NA, Glick RE** (1994) Biochemical and molecular basis for impairment of photosynthetic potential. *Photosynthesis Research* **39**: 453-462

- Pellinen R, Palva T, Kangasjärvi J** (1999) Subcellular localization of ozone-induced hydrogen peroxide production in birch (*Betula pendula*) leaf cells. *The Plant Journal* **20**: 349-356
- Peterson RB** (1989) Partitioning of noncyclic photosynthetic electron transport to O₂-dependent dissipative processes as probe by fluorescence and CO₂ exchange. *Plant Physiology* **90**: 1322-1328
- Rakonczay Z** (1997) Characterizing the respiration of stems and roots of three hardwood species in Great Smoky Mountains. Ph.D. Dissertation, Virginia Polytechnic Institute and State University
- Rebbeck J** (1996) Chronic ozone effects on three northeastern hardwood species: growth and biomass. *Canadian Journal of Forest Research* **26**: 1788-1798
- Reich PB** (1987) Quantifying plant response to ozone: a unifying theory. *Tree Physiology* **3**: 63-91
- Reichenauer T, Bolhar-Nordenkamp HR, Soja G** (1997) Chronology of changes within the photosynthetic apparatus of *Populus nigra* under ozone stress. *Phyton* **37**: 245-250
- Reiling K and Davison AW** (1994) Effects of exposure to ozone at different stages in the development of *Plantago major* L. chlorophyll fluorescence and gas exchange. *New Phytologist* **128**: 509-514
- Reiling K and Davison AW** (1992) The response of native, herbaceous species to ozone: growth and fluorescence screening. *New Phytologist* **120**:29–37
- Ribas A, Filella I, Gimeno BS, Penuelas J** (1998) Evaluation of tobacco cultivars as bioindicators and biomonitors of ozone phytotoxic levels in Catalonia. *Water, Air, and Soil Pollution*. **107**: 347-365
- Rohacek K and Bartak M** (1999) Technique of the modulated chlorophyll fluorescence: Basic concepts, useful parameters, and some applications. *Photosynthetica* **37**: 339-363

- Rowland-Bamford AJ, Coghlan S, Lea PJ** (1989) Ozone-induced changes in CO₂ assimilation, O₂ evolution and chlorophyll a fluorescence transients in barley. *Environmental Pollution* **59**: 129-140
- Runeckles VC and Chevone BI** (1992) Crop responses to ozone. *In* Surface Level Ozone Exposures and Their Effects on Vegetation. Lewis Publisher Inc., Chelsea, MI, pp 189-270
- Runeckles VC and Krupa SV** (1994) The impact of UV-B radiation and ozone on terrestrial vegetation. *Environmental Pollution* **83**: 191-213
- Saitanis CJ and Karandinis MG** (2002) Effects of ozone on tobacco (*Nicotiana tabacum* L.) varieties. *Journal of Agronomy and Crop Science* **188**: 51-58
- Samuelson LJ** (1994) Ozone exposure responses of black cherry and red maple seedlings. *Environmental and Experimental Botany* **34**: 355-362
- Sasek TW and Richardson CJ** (1989) Effects of chronic doses of ozone on loblolly pine: Photosynthetic characteristics in the third growing season. *Forest Science* **35**: 745
- Schaub M, Skelly JM, Steiner KC, Davis DD, Pennypacker SP, Zhang J, Ferdinand JA, Savage JE, Stevenson RE** (2003) Physiological and foliar injury responses of *Prunus serotina*, *Fraxinus americana*, and *Acer rubrum* seedlings to varying soil moisture and ozone. *Environmental Pollution* **124**: 307-320
- Schaub M, Skelly JM, Zhang JW, Ferdinand JA, Savage JE, Stevenson RE, Davis DD, Steiner KC** (2005) Physiological and foliar symptom response in the crowns of *Prunus serotina*, *Fraxinus americana* and *Acer rubrum* canopy trees to ambient ozone under forest conditions. *Environmental Pollution* **133**: 552-567
- Scheidegger C and Schroeter B** (1995) Effects of ozone fumigation on epiphytic macro lichens: Ultrastructure, CO₂ gas exchange and chlorophyll fluorescence. *Environmental Pollution* **88**: 345-354

- Schmieden U, Schneider S, Wild A** (1993) Glutathione status and glutathione reductase activity in spruce needles of healthy and damaged trees at two mountain sites. *Environmental Pollution* **82**: 239-244
- Schraudner M, Langebartels C, Sandermann H** (1997) Changes in biochemical status of plant cells induced by the environmental pollutant ozone. *Physiologia Plantarum* **100**: 274-280
- Schreiber U, Schliwa U, Bilger W** (1986) Continuous recording of photochemical and non-photochemical chlorophyll fluorescence quenching with a new type of a modulated fluorometer. *Photosynthesis Research* **10**: 51-62
- Schreiber U, Vidaver W, Runeckles VC, Rosen P** (1978) Chlorophyll fluorescence assay for ozone injury in intact plants. *Plant Physiology* **61**: 80-84
- Shavin S, Maurer S, Matyssek R, Bilger W, Scheidegger C** (1999) The impact of ozone fumigation and fertilization on chlorophyll fluorescence of birch leaves (*Betula pendula*). *Trees* **14**: 10-16
- Showman RE** (1991) A comparison of ozone injury to vegetation during moist and drought years. *Journal of the Air and Waste Management Association* **41**: 63-64
- Simini M, Skelly JM, Davis DD, Savage JE, Comrie AC** (1992) Sensitivity of four hardwood species to ambient ozone in northcentral Pennsylvania. *Canadian Journal of Forest Research* **22**: 1789-1799
- Skarby L, Ro-Poulsen H, Wellburn FAM, Sheppard LJ** (1998) Impact of ozone on forest: A European perspective. *New Phytologist* **139**: 109-122
- Skelly JM** (2000) Tropospheric ozone and its importance to forests and natural plant communities of the northeastern United States. *Northeastern Naturalist* **7**: 221-236
- Skelly JM, Innes JL, Snyder KR, Savage JE, Hog C, Landolt W, P. B** (1998) Investigations of ozone induced injury in forests of southern Switzerland: Field surveys and open-top chamber experiments. *Chemosphere* **35**: 995-1000

- Skelly JM, Savage JE, Bauer MDL, Alvarado D** (1997) Observations of ozone-induced foliar injury on black cherry (*Prunus serotina*, var. Capuli) within the Desierto de los Leones National Park, Mexico City. *Environmental Pollution* **95**: 155-158
- Soja G, Pfeifer U, Soja AM** (1998) Photosynthetic parameters as early indicators of ozone injury in apple leaves. *Physiologia Plantarum* **104**: 639-645
- Tausz M, Šircelj H and Grill D** (2004) The glutathione system as a stress marker in plant ecophysiology: Is a stress-response concept valid? *Journal of Experimental Botany* **55**:1955-1962
- Tenga AZ, Hale B, Ormrod DP** (1993) Growth responses of young cuttings of *Populus deltoides* X *nigra* to ozone in controlled environments. *Canadian Journal of Forest Research* **23**: 854-858
- Torsethaugen G, Pitcher LH, Zilinskas BA, Pell EJ** (1997) Overproduction of ascorbate peroxidase in the tobacco chloroplast does not provide protection against ozone. *Plant Physiology* **114**: 529-537
- USEPA** (1996) Air quality criteria for ozone and related photochemical oxidants. Volume 2 EPA/600/AP-95/004 aF-cF
- Van Buuren ML, Guidi L, Fornale S, Ghetti F, Franceschetti M, Soldatini GF, Bagni N** (2002) Ozone-response mechanisms in tobacco: implications of polyamine metabolism. *New Phytologist* **156**: 389-398
- Van der Eerden LJ, Tonneijck AEG, Wijnands JHM** (1988) Crop loss due to air pollution in the Netherlands. *Environmental Pollution* **53**: 365-376
- von Caemmerer, S. and Farquhar GD** (1981) Some relationship between biochemistry of photosynthesis and the gas exchange of leaves. *Planta* **153**:376-387

- VanderHeyden D, Skelly J, Innes J, Hog C, Zhang J, Landolt W, Bleuler P** (2001) Ozone exposure thresholds and foliar injury on forest plants in Switzerland. *Environmental Pollution* **111**: 321-331
- Vollenweider P, Woodcock H, Kelty MJ, Hofer R-M** (2003) Reduction of stem growth and site dependency of leaf injury in Massachusetts black cherries exhibiting ozone symptoms. *Environmental Pollution* **125**: 467-480
- Wellburn AR** (1997) Environmental factors and genotypic changes in lipids contribute to the winter hardiness of Norway spruce (*Picea abies*). *New Phytologist* **135**: 115-121
- Wohlgemuth H, Mittelstrass K, Kschieschan S, Bender J, Weigel H-J, Overmyer K, Kangasjärvi J, Sandermann H, Langebartels C** (2002) Activation of an oxidative burst in a general feature of sensitive plants exposed to the air pollutant ozone. *Plant, Cell and Environment* **25**: 717-726
- Yun SC and Laurence JA** (1999) The response of sensitive and tolerant clones of *Populus tremuloides* to dynamic ozone exposure under controlled environmental conditions. *New Phytologist* **143**: 305-313
- Yuska DE, Skelly JM, Ferdinand JA, Stevenson RE, Savage JE, Mulik JD, Hines A** (2003) Use of bioindicators and passive sampling devices to evaluate ambient ozone concentrations in northcentral Pennsylvania. *Environmental Pollution* **125**: 71-80

Appendix - I. Tables

Table A.1 Gas exchange analysis was conducted during the growing seasons of 2000 to 2002 at three different sites MTR, APL, and HRC. Various photosynthetic activities (Pn_{MAX} , $\mu\text{mol CO}_2 \text{ m}^{-2}\text{s}^{-1}$ at $900 \mu\text{mol m}^{-2}\text{s}^{-1}$; g_s , $\text{mol H}_2\text{O m}^{-2}\text{s}^{-1}$; C_i , ppm; ΦCO_2 , $\mu\text{mol quanta}^{-1}$; and ΦCE) on the 3rd basal leaf were compared between tolerant (T) and sensitive (S) black cherry. Values are mean \pm s.d.

			May 2000	June 2000		June 2001		July 2000		July 2002		August 2000		August 2002		September 2000		September 2001		
Pn_{MAX}	MTR	T	8.21 \pm 0.12	8.34 \pm 0.25	–	–	–	8.53 \pm 1.66	–	–	–	10.2 \pm 0.56	–	–	–	7.41 \pm 0.84	–	–	–	
		S	10.5 \pm 0.26	10.9 \pm 0.1	–	–	–	9.57 \pm 0.44	–	–	–	6.99 \pm 0.63	–	–	–	3.58 \pm 2.02	–	–	–	
	APL	T	–	–	8.66 \pm 0.33	10.4 \pm 1.11	–	–	8.33 \pm 0.23	–	–	–	–	–	–	–	–	10.4 \pm 1.09	–	–
		S	–	–	9.28 \pm 0.59	10.2 \pm 0.47	–	–	8.08 \pm 0.92	–	–	–	–	–	–	–	–	6.67 \pm 0.08	–	–
	HRC	T	7.42 \pm 0.42	10.9 \pm 1.50	8.36 \pm 0.22	9.18 \pm 1.13	–	–	9.81 \pm 0.42	11.3 \pm 2.11	–	–	9.77 \pm 0.93	9.77 \pm 0.93	–	–	8.07 \pm 0.77	11.8 \pm 0.75	–	–
		S	9.16 \pm 0.67	11.3 \pm 0.94	8.86 \pm 0.47	8.48 \pm 1.20	–	–	8.93 \pm 0.25	8.59 \pm 1.49	–	–	7.26 \pm 0.93	7.35 \pm 0.68	–	–	2.85 \pm 0.67	5.62 \pm 0.41	–	–
g_s	MTR	T	0.132 \pm 0.02	0.238 \pm 0.02	–	–	–	0.199 \pm 0.07	–	–	–	0.215 \pm 0.03	–	–	–	0.174 \pm 0.01	–	–	–	
		S	0.153 \pm 0.04	0.299 \pm 0.01	–	–	–	0.24 \pm 0.01	–	–	–	0.142 \pm 0.01	–	–	–	0.112 \pm 0.04	–	–	–	
	APL	T	–	–	0.142 \pm 0.01	0.05 \pm 0.005	–	–	0.02 \pm 0.001	–	–	–	–	–	–	–	–	0.232 \pm 0.05	–	–
		S	–	–	0.241 \pm 0.06	0.04 \pm 0.008	–	–	0.03 \pm 0.001	–	–	–	–	–	–	–	–	0.181 \pm 0.03	–	–
	HRC	T	0.10 \pm 0.01	0.26 \pm 0.04	0.246 \pm 0.01	0.04 \pm 0.007	–	–	0.16 \pm 0.06	0.247 \pm 0.06	–	–	0.22 \pm 0.01	0.22 \pm 0.01	–	–	0.21 \pm 0.02	0.22 \pm 0.04	–	–
		S	0.17 \pm 0.02	0.30 \pm 0.02	0.284 \pm 0.02	0.04 \pm 0.009	–	–	0.21 \pm 0.04	0.233 \pm 0.03	–	–	0.21 \pm 0.04	0.106 \pm 0.01	–	–	0.22 \pm 0.04	0.20 \pm 0.01	–	–
C_i	MTR	T	223 \pm 14	267 \pm 7	–	–	–	263 \pm 9	–	–	–	255 \pm 8	–	–	–	268 \pm 5	–	–	–	
		S	228 \pm 3	262 \pm 7	–	–	–	257 \pm 3	–	–	–	249 \pm 15	–	–	–	289 \pm 17	–	–	–	
	APL	T	–	–	224 \pm 3	–	–	–	299 \pm 4	–	–	–	–	–	–	–	–	244 \pm 8	–	–
		S	–	–	257 \pm 21	–	–	–	313 \pm 5	–	–	–	–	–	–	–	–	263 \pm 4	–	–
	HRC	T	206 \pm 9	254 \pm 5	258 \pm 9	–	–	200 \pm 10	–	–	–	278 \pm 5	–	–	–	273 \pm 4	219 \pm 13	–	–	–
		S	234 \pm 7	259 \pm 4	276 \pm 7	–	–	256 \pm 6	–	–	–	298 \pm 10	–	–	–	308 \pm 10	278 \pm 1	–	–	–
ΦCO_2	HRC	T	0.050 \pm 0.002	–	0.049 \pm 0.002	0.057 \pm 0.006	–	0.048 \pm 0.002	0.061 \pm 0.002	–	–	0.049 \pm 0.002	0.059 \pm 0.0001	–	–	0.039 \pm 0.002	0.058 \pm 0.0009	–	–	
		S	0.046 \pm 0.003	–	0.053 \pm 0.004	0.063 \pm 0.005	–	0.047 \pm 0.001	0.052 \pm 0.001	–	–	0.042 \pm 0.002	0.051 \pm 0.003	–	–	0.031 \pm 0.001	0.053 \pm 0.0005	–	–	
ΦCE	HRC	T	–	–	–	0.044 \pm 0.002	–	–	0.035 \pm 0.005	–	–	–	0.039 \pm 0.007	–	–	–	–	–	–	
		S	–	–	–	0.039 \pm 0.005	–	–	0.026 \pm 0.005	–	–	–	0.023 \pm 0.003	–	–	–	–	–	–	

Table A.2 Chlorophyll fluorescence in the dark-adapted state (Fm, maximum fluorescence; Fo, initial fluorescence; and Fv/Fm, maximum photochemical efficiency), quantum yield for PSII (Φ_{PSII}), maximum electron transport rate (ETR, $\mu\text{mol electron m}^{-2} \text{s}^{-1}$ at $950 \mu\text{mol m}^{-2} \text{s}^{-1}$), and quenching coefficients (qP, photochemical quenching; qN, non-photochemical quenching) on the 3rd leaf of black cherry during growing season of 2000 at HRC. Values are means \pm s.d. Asterisks indicate significant differences between cultivars * at $P < 0.05$ and ** at $P < 0.01$

	<i>June</i>		<i>July</i>		<i>August</i>		<i>September</i>	
	<u>Sensitive</u>	<u>Tolerant</u>	<u>Sensitive</u>	<u>Tolerant</u>	<u>Sensitive</u>	<u>Tolerant</u>	<u>Sensitive</u>	<u>Tolerant</u>
Fm	1.516 \pm 0.019	1.495 \pm 0.167	1.302 \pm 0.037	1.491 \pm 0.107**	1.250 \pm 0.139	1.288 \pm 0.079	1.604 \pm 0.193	1.815 \pm 0.055
Fo	0.247 \pm 0.007	0.252 \pm 0.007	0.264 \pm 0.017	0.238 \pm 0.007*	0.252 \pm 0.016	0.237 \pm 0.008	0.388 \pm 0.019	0.308 \pm 0.016**
Fv/Fm	0.837 \pm 0.005	0.830 \pm 0.022	0.797 \pm 0.013	0.840 \pm 0.010**	0.796 \pm 0.019	0.815 \pm 0.013	0.755 \pm 0.039	0.831 \pm 0.008*
Φ_{PSII}	0.385 \pm 0.059	0.438 \pm 0.035	0.284 \pm 0.027	0.263 \pm 0.011	0.323 \pm 0.019	0.364 \pm 0.026	0.197 \pm 0.079	0.428 \pm 0.020**
ETR	168 \pm 26	194 \pm 15	133 \pm 10	123 \pm 6	155 \pm 7	171 \pm 14	102 \pm 42	226 \pm 11**
qP	–	–	0.716 \pm 0.102	0.633 \pm 0.081	0.804 \pm 0.112	0.722 \pm 0.085	0.926 \pm 0.128	0.843 \pm 0.031
qN	–	–	0.805 \pm 0.066	0.815 \pm 0.049	0.777 \pm 0.038	0.675 \pm 0.075	0.907 \pm 0.073	0.713 \pm 0.018**

– Data not available

Table A.3 Chlorophyll fluorescence in the dark-adapted state (Fm, maximum fluorescence; Fo, initial fluorescence; and Fv/Fm, maximum photochemical efficiency), quantum yield for PSII (Φ_{PSII}), maximum electron transport rate (ETR, $\mu\text{mol electron m}^{-2} \text{s}^{-1}$ at $950 \mu\text{mol m}^{-2} \text{s}^{-1}$), and quenching coefficients (qP, photochemical quenching; qN, non-photochemical quenching) on the 3rd leaf of black cherry during the growing season of 2001 at HRC. Values are means \pm s.d. Asterisks indicate significant differences between cultivars * at $P < 0.05$ and ** at $P < 0.01$

	<i>June</i>		<i>July</i>		<i>August</i>		<i>September</i>	
	<u>Sensitive</u>	<u>Tolerant</u>	<u>Sensitive</u>	<u>Tolerant</u>	<u>Sensitive</u>	<u>Tolerant</u>	<u>Sensitive</u>	<u>Tolerant</u>
Fm	1.368 \pm 0.109	1.417 \pm 0.052	1.400 \pm 0.175	1.406 \pm 0.107	1.439 \pm 0.176	1.374 \pm 0.036	1.306 \pm 0.041	1.254 \pm 0.166
Fo	0.245 \pm 0.022	0.235 \pm 0.015	0.261 \pm 0.040	0.232 \pm 0.013**	0.294 \pm 0.042	0.256 \pm 0.017**	0.289 \pm 0.003	0.241 \pm 0.001**
Fv/Fm	0.820 \pm 0.016	0.830 \pm 0.011	0.814 \pm 0.022	0.834 \pm 0.013*	0.796 \pm 0.008	0.814 \pm 0.012**	0.779 \pm 0.004	0.805 \pm 0.027*
Φ_{PSII}	–	–	0.207 \pm 0.038	0.290 \pm 0.061	0.132 \pm 0.009	0.185 \pm 0.001	0.097 \pm 0.002	0.225 \pm 0.034**
ETR	–	–	90 \pm 19	121 \pm 26	58 \pm 5	84 \pm 1**	47 \pm 1	105 \pm 17**
qP	–	–	0.902 \pm 0.099	0.626 \pm 0.013**	0.664 \pm 0.025	0.571 \pm 0.087	0.547 \pm 0.017	0.654 \pm 0.025**
qN	–	–	0.944 \pm 0.014	0.814 \pm 0.064*	0.930 \pm 0.004	0.865 \pm 0.017**	0.930 \pm 0.010	0.864 \pm 0.035*

– Data not available

Table A.4 Chlorophyll fluorescence in the dark-adapted state (F_m , maximum fluorescence; F_o , initial fluorescence; and $F_v \pm / F_m$, maximum photochemical efficiency), quantum yield for PSII (Φ_{PSII}), maximum electron transport rate (ETR, $\mu\text{mol electron m}^{-2} \text{s}^{-1}$ at $950 \mu\text{mol m}^{-2} \text{s}^{-1}$), quenching coefficients (qP, photochemical quenching; qN, non-photochemical quenching), and chlorophyll concentrations on the 3rd leaf of black cherry during the growing season of 2002 at HRC. Values are means \pm s.d. Asterisks indicate significant differences between phenotypes. * at $P < 0.05$ and ** at $P < 0.01$

	<i>June</i>		<i>July</i>		<i>August</i>	
	<u>Sensitive</u>	<u>Tolerant</u>	<u>Sensitive</u>	<u>Tolerant</u>	<u>Sensitive</u>	<u>Tolerant</u>
F_m	1.117 \pm 0.084	1.019 \pm 0.125	1.068 \pm 0.014	1.05 \pm 0.100	0.892 \pm 0.129	1.161 \pm 0.079
F_o	0.202 \pm 0.013	0.158 \pm 0.008*	0.224 \pm 0.017	0.195 \pm 0.017	0.215 \pm 0.025	0.207 \pm 0.016
F_v/F_m	0.819 \pm 0.002	0.844 \pm 0.012	0.789 \pm 0.018	0.814 \pm 0.002	0.758 \pm 0.009	0.822 \pm 0.003*
Φ_{PSII}	0.219 \pm 0.076	0.332 \pm 0.043	0.191 \pm 0.036	0.336 \pm 0.051**	0.259 \pm 0.059	0.359 \pm 0.001*
ETR	84 \pm 28	117 \pm 14	77 \pm 13	128 \pm 22**	99 \pm 20	139 \pm 9*
qP	0.809 \pm 0.168	0.705 \pm 0.054	0.897 \pm 0.171	0.665 \pm 0.099	0.872 \pm 0.131	0.877 \pm 0.123
qN	0.901 \pm 0.055	0.803 \pm 0.053*	0.926 \pm 0.021	0.784 \pm 0.016**	0.887 \pm 0.039	0.867 \pm 0.076

Appendix – II. Symbols and units

P_n	Net CO ₂ assimilation rate ($\mu\text{mol CO}_2 \text{ m}^{-2} \text{ s}^{-1}$)
P_{nMAX}	Maximum net CO ₂ assimilation rate ($\mu\text{mol CO}_2 \text{ m}^{-2} \text{ s}^{-1}$ at $900 \mu\text{mol m}^{-2} \text{ s}^{-1}$ PAR)
A_{SAT}	Net CO ₂ assimilation rate at light saturation ($\mu\text{mol CO}_2 \text{ m}^{-2} \text{ s}^{-1}$)
g_s	Stomatal conductance ($\text{mmol H}_2\text{O m}^{-2} \text{ s}^{-1}$ or $\text{mol H}_2\text{O m}^{-2} \text{ s}^{-1}$)
Φ_{CO_2}	Apparent quantum yield of CO ₂ assimilation
Φ_{PSII}	Apparent quantum efficiency of PSII
Φ_{CE}	Carboxylation efficiency
R_D	Daytime dark respiration ($\mu\text{mol CO}_2 \text{ m}^{-2} \text{ s}^{-1}$)
LCP	Light compensation point ($\mu\text{mol m}^{-2} \text{ s}^{-1}$ PAR)
PAR	Photosynthetically active radiation ($\mu\text{mol m}^{-2} \text{ s}^{-1}$)
F_o	Minimum chlorophyll fluorescence
F_m	Maximum chlorophyll fluorescence
F_v	Variable chlorophyll fluorescence (F _m -F _o)
F_v/F_m	Maximum photochemical efficiency
ETR	Electron transport rate
qP	Photochemical quenching coefficients
qN	Non-photochemical quenching coefficients

Vita

Myoung-Hui Yun

Education

- | | |
|-----------|--|
| 1997-2007 | Ph. D., Plant Physiology
Department of Plant Pathology, Physiology, and Weed Science
Virginia Tech
Blacksburg, VA |
| 1995-1997 | M.S., Plant Physiology and Environmental Ecology
Department of Biological Science
Myongji University
Seoul, Korea |
| 1991-1995 | B.S., Biology
Department of Biology
Myongji University |

Research Experience

- | | |
|-----------|---|
| 2003-2004 | Laboratory Technician in Air Pollution Lab, Department of Plant Pathology, Physiology, and Weed Science, Virginia Tech. |
| 2000-2003 | Graduate Research Assistant, Department of Plant Pathology, Physiology, and Weed Science, Virginia Tech. |
| 1999-2000 | Laboratory Specialist in Air pollution Lab, Department of Plant Pathology, Physiology, and Weed Science, Virginia Tech. |
| 1998-1999 | Laboratory Technician in Air Pollution Lab, Department of Plant Pathology, Physiology, and Weed Science, Virginia Tech. |

Teaching Experience

- | | |
|-----------|---|
| 2000-2001 | PPWS 3514 Plant Physiology Lab, Department of Plant Pathology, Physiology, and Weed Science, Virginia Tech. |
| 1995-1996 | Biology Lab, Department of Biological Science, Myongji University |
| 1996-1996 | Ecology Lab, Department of Biological Science, Myongji University |

Presentations

Regional

“Ozone Effects on Photosynthesis and PSII Function in Plants with Contrasting Pollutant Sensitivities” Annual meeting of American society of Plant Physiologist, North Carolina

Sate University, NC, December 6-7,2000

“Ozone Effects on Photosynthesis and PSII Function in Tobacco with Contrasting Pollutant Sensitivities” Korean Scientists and Engineers Association Southern Chapter Conference, North Carolina State University, NC, December 4, 1999

Local

“Ozone Effects on Photosynthesis and PSII Function in Tobacco with Contrasting Pollutant Sensitivities” Korean Scientists and Engineers Association Southern Chapter Conference, Virginia Tech, VA, October, 2002

Publications

Yun, M. H. (2006) Effects of High Ozone on CO₂ Assimilation and PSII function in Two Tobacco cultivars with different sensitivities. Journal of Korean Atmospheric Environments **22**: 89-98

Research Interests

Air pollutant effects on plants

- Photosynthesis and chlorophyll fluorescence responses of tolerant and sensitive plants to ozone under controlled laboratory conditions.
- The effects of ambient ozone concentrations on photosynthesis and chlorophyll fluorescence in tolerant and sensitive forest tree species.

Professional Affiliations

American Society of Plant Biologists (ASPB)

Ecological Society of America (ESA)

Korean Society for Atmospheric Environment (KSAE)